MASARYK UNIVERSITY

FACULTY OF SCIENCE

Time control and reconstruction of paleoenvironmental changes from Paleozoic carbonate record

Habilitation Thesis

TOMÁŠ KUMPAN

Department of Geological Sciences

Brno 2026

MUNI
SCI

Bibliographic record

Author: TOMÁŠ KUMPAN
Faculty of Science
Masaryk University
Department of Geological Sciences

Title of Thesis: Time control and reconstruction of paleoenvironmental changes from Paleozoic carbonate record

Year: 2026

Number of Pages: 71 + 364

Keywords: Stratigraphy, Geochemistry, Conodonts, Trace elements, Ordovician, Devonian, Carboniferous, Hangenberg Crisis, red limestones

Abstract

This Habilitation thesis presents my research from the past ten years (2016–2026), focused on multidisciplinary stratigraphy and paleoenvironmental reconstruction from Paleozoic carbonate rocks. The thesis is a commentary on fifteen selected publications, organized into two thematic parts.

The first part (Advances in Devonian and Carboniferous Stratigraphy) addresses several stratigraphic problems and their solutions. The first topic concerns the ongoing reappraisal of the Devonian-Carboniferous boundary Global Standard Section and Point. The applicability of the *Protognathodus kockeli* conodont Zone and detrital element chemostratigraphy as tools for a revised multicriteria boundary definition were tested across sections in the Europe and North America. The second topic addresses the refinement of lower Tournaisian stratigraphy through revision of *Siphonodella* conodont taxonomy and biostratigraphy, and the identification of three small-scale carbon isotope excursions in the Moravosilesian Basin. These excursions provide tool for interregional correlation in Paleotethys Realm and potentially beyond.

The second part (Element geochemistry in Paleoenvironmental reconstruction) presents commentary to series of case studies on paleoenvironmental reconstruction from Ordovician, Devonian, and Carboniferous limestones across Europe and Asia. Bulk (EDXRF, ICP-OES/MS) and *in situ* (LA-ICP-MS) geochemistry approaches were combined in research of deposits from redox-contrasting settings. The third topic of the thesis focuses on the Devonian-Carboniferous Hangenberg Crisis, documenting paleoredox oscillations, and the role of continental runoff, magmatic activity, and basin restriction in driving marine anoxia. The last topic examines marine red limestones from the Ordovician (Baltoscandia, South China) and Devonian (Prague Basin, Montagne Noire), reconstructing the processes responsible for Fe-oxide precipitation and early diagenetic trace element redistribution. A principal methodological contribution of the second part of the thesis is combination of bulk geochemical analyses with *in situ* LA-ICP-MS microgeochemistry. The latter method enables to explore individual carbonate components, which reveals geochemical contrasts between colour and fabric domains that are mixed in bulk-rock data.

The Habilitation thesis demonstrates that integration of conodont biostratigraphy and multi-proxy geochemistry provides a robust framework for both stratigraphic correlations and paleoenvironmental interpretations. Reliable reconstruction from carbonate archives, however, ultimately depends on matching the scale of resolution of the analytical method to the scale of the processes under investigation.

Declaration

I declare that I have prepared my thesis independently using the information sources cited in the thesis. AI-assisted language tool (Claude, Anthropic) was used for English language corrections and improvement.

Acknowledgements

I would like to take this opportunity to thank my beloved wife Simona, who supported and motivated me throughout this journey and never stopped believing in me. I would also like to express my gratitude to my family, my mother, father, sister and grandparents, as well as all friends for the selfless support.

I am especially indebted to my mentors Jirka Kalvoda and Ondra Bábek for their kind guidance during my graduate and postgraduate research, and friendly collaboration until now. My thanks also go to my colleagues, with whom I have worked closely over the years and who have contributed greatly to my scientific development, above all: Stáňa Vodrážková, Jirka Frýda and Markéta Holá. I would like to thank my colleague Petr Zaunstöck for his skilled preparation of polished sections, which contributed significantly to the results presented here.

Last but not least, I wish to express my gratitude to all colleagues who have contributed as co-authors to any of our joint publications, whether included in this thesis or not, particularly Sandra Kaiser, Thomas Becker, Sven Hartenfels, Axel Munnecke, Carlo Corradini, Claudia Spalletta, Catherine Girard, Wenkun Qie, Tomáš Matys Grygar, Radek Vodrážka, Vojta Cígler, and Renata Čopjaková. This body of work would not exist without them.

Table of Contents

Abbreviations **11**

1 Introduction **13**

2 Advances in Devonian and Carboniferous Stratigraphy **21**

2.1 Topic A: Redefinition of the Devonian-Carboniferous System Boundary...21

2.2 Topic B: Advances in lower Tournaisian stratigraphy.....30

3 Element geochemistry in Paleoenvironmental reconstruction: from black to red deposits **38**

3.1 Topic C: Hangenberg Crisis and its anoxic black deposits.....39

3.2 Topic D: Geochemistry of Paleozoic Red Iron-rich Marine Sediments 48

4 Conclusions and Outlook **59**

Bibliography **61**

Appendix A Attached Commented Articles **72**

Abbreviations

DCB	Devonian–Carboniferous Boundary
EDXRF	Energy Dispersive X-ray Fluorescence
EF	Enrichment Factor
FO	First Occurrence
GSSP	Global Stratotype Section and Point
HBSE	Hangenberg Black Shale Event
HSE	Hangenberg Sandstone Event
ICP-MS	Inductively Coupled Plasma Mass Spectrometry
ICP-OES	Inductively Coupled Plasma Optical Emission Spectrometry
LA-ICP-MS	Laser Ablation Inductively Coupled Plasma Mass Spectrometry
LTICE	Lower Tournaisian Isotopic Carbon Excursion
MRBs	Marine Red Beds
PAAS	Post-Archean Australian Shale
REE	Rare Earth Elements
SEM	Scanning Electron Microscopy
SEM-EDX	SEM with Energy Dispersive X-ray analysis
SLE	Stockum Limestone Event
TICE	mid-Tournaisian Isotopic Carbon Excursion
UCC	Upper Continental Crust
V-PDB	Vienna Pee Dee Belemnite – isotopic standard
XRD	X-ray Diffraction

1 Introduction

Understanding the timing and drivers of past environmental changes is one of the fundamental objectives in the geosciences. Investigation of these changes recorded in geological archives allows us to understand the dynamics of natural processes over long time series. Sedimentary rocks provide the most continuous archives of geological events, climate variability, biogeochemical cycles, and ecosystem turnovers, and are crucial for such research. Paleoenvironmental interpretation of sedimentary record, however, fundamentally depends on reliable time control, placing geological events into a chronological framework. Stratigraphy and geochronology provide numerous tools for resolving the temporal dimension of the geological record.

My stratigraphic a paleoenvironmental research focuses on Paleozoic carbonate sediments, which represent both excellent archives and a methodological challenge. The high preservation potential and fossil content in biogenic limestones make them ideal for stratigraphic and paleoenvironmental investigation of deep-time Palaeozoic environments and ecosystems. On the other hand, their diagenetic overprint and tectonic deformation often complicate application of high-resolution astrochronology, and radiometric dating remains limited by the rarity of datable tuffs. In many cases, biostratigraphy complemented by chemostratigraphy remains the most widely applicable approach for time control in geologically mature Paleozoic rocks. In my research, I integrate conodont biostratigraphy with carbon isotope and elemental chemostratigraphy to establish stratigraphic framework for palaeoenvironmental and event reconstructions. My approach of paleoenvironmental analysis combines methods of carbonate sedimentology with multi-proxy geochemistry.

This thesis provides synthesis of my research conducted over the last ten years (2016-2026), focusing on Ordovician, Devonian and Carboniferous carbonate successions of Europe, Asia, and North America (Fig. 1). I have selected 15 from a total of 25 authored or co-authored papers in international journals since the completion of my doctoral degree. Commentary can be naturally structured into two thematic parts, each presenting my results in two general topics.

In **the first part *Advances in Devonian and Carboniferous Stratigraphy*** [**Papers 1–7**], I address stratigraphic problems related to redefinition of DCB and stratigraphic subdivision of the lower Tournaisian. Results of testing two criteria proposed for the redefinition of the DCB are commented in **Topic A *Redefinition of the Devonian-Carboniferous System Boundary***: the evolutionary lineage of *Protognathodus collinsoni–kockeli* as a biostratigraphic tool [**Papers 1 and 2**], and element chemostratigraphy proxy to identify the major regression associated with the Hangenberg Crisis across various depositional settings [**Papers 2–4**]. **Topic B *Revised lower Tournaisian conodont taxonomy and biostratigraphy*** provides commentary to my work

on refinement of the lower Tournaisian stratigraphy by study of conodont taxonomy and biostratigraphy [**Papers 5 and 6**] and carbon isotope chemostratigraphy [**Paper 7**].

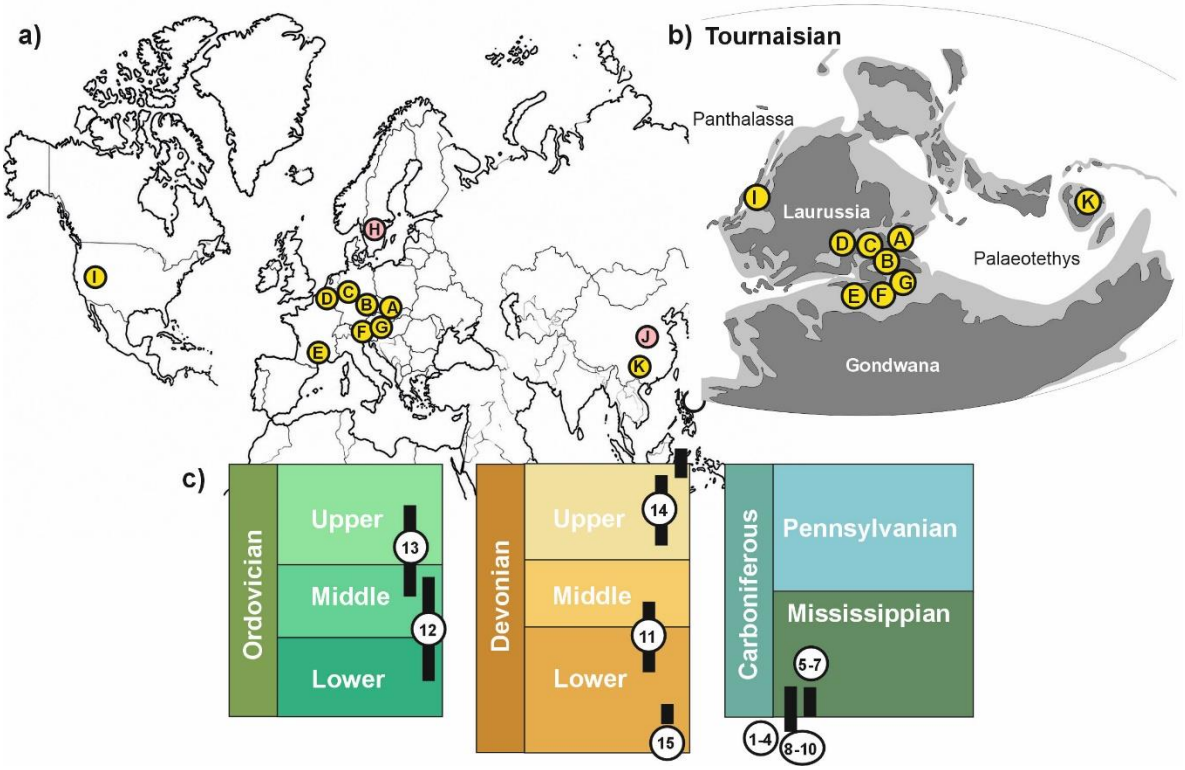

Figure 1. Areas studied and sampled for the research presented in the habilitation thesis. (**a**) Geographic location of all study areas: A - Moravian Karst (Moravosilesian Basin), B – Barrandian (Prague Basin), C - Rhenish Slate Mountains (Rhenish Massif), D – Ardennes (Namur-Dinant Basin), E - Montagne Noire, F - Carnic Alps, G - Graz Paleozoic, H – Västergötland, I - Confusion Range, J - Yangtze Platform, K – Guangxi Platform, pink circles – Ordovician rocks, yellow circles – Devonian and/or Carboniferous; (**b**) approximate paleogeographic positions of areas with studied Devonian and/or Carboniferous sections (Tournaisian situation, modified after Blakey 2012); (**c**) stratigraphic intervals covered by the annotated studies (circled numbers refer to annotated **Papers 1–15**).

In the **second part *Element geochemistry in Paleoenvironmental reconstruction: from black to red deposits*** [**Papers 8–15**], I synthesize several case studies on palaeoenvironmental reconstruction based on trace and REE elements analysis of Ordovician, Devonian, and Carboniferous limestones. I have used element geochemistry to investigate various paleoenvironmental signals and diagenetic processes in contrasting sedimentary settings: organic-rich black deposits of the Hangenberg Crisis (**Topic C; *Hangenberg Crisis and its anoxic black deposits*; Papers 8-10**) and iron-rich red carbonates of the selected Ordovician and Devonian stratigraphic intervals (**Topic D**; **Geochemistry of Paleozoic Red Iron-rich Marine Sediments; Papers 11-15**). The selected papers show development of my methodological approach from

study of bulk geochemical information across stratigraphic sections to combination with *in situ* microgeochemistry. The higher resolution of microgeochemistry provide view on the record of processes related to microenvironments or high-frequency paleoenvironmental changes, which are mixed in bulk samples, and allow more robust reconstructions. The multivariate datasets show, that the geochemical record is highly complex, and combination with paleontological and sedimentological approaches is necessary.

The papers for which the habilitation thesis serves as a commentary are included in **Appendix A** and referred to throughout the text according to the numbering given below (e.g., **Paper 1**). My specific contributions to each paper are detailed therein:

[1] KAISER, I, **Tomas KUMPAN** and Michael W. RASSER. High-resolution conodont biostratigraphy in two key sections from the Carnic Alps (Grune Schneid) and Graz Paleozoic (Trolp) - implications for the biozonation concept at the DCB. *Newsletters on Stratigraphy* [online]. 2020, **53**(3), 249–274. ISSN 0078-0421. Available at: doi:10.1127/nos/2019/0520

According to AIS GEOLOGY – SCIE Q1

Author's contribution to the publication: I participated in the analysis of part of the conodont material and in the development of the research design, and contributed to manuscript writing.

Experimental work (%)	Supervision (%)	Manuscript (%)	Research direction (%)
0	0	40	40

[2] KUMPAN, Tomas*(corresponding author)*, Jiri KALVODA, Ondrej BABEK, Tomas Matys GRYGAR and Jiri FRYDA. The DCB in the Moravian Karst (Czech Republic). Palaeobiodiversity and Palaeoenvironments [online]. 2021, **101**(2), 473–485. ISSN 1867-1608. Available at: doi:10.1007/s12549-019-00409-z

According to AIS PALEONTOLOGY – SCIE Q3

Author's contribution to the publication: I led the author collective in preparation of this review paper, which includes new data, for a special volume on the global Devonian–Carboniferous boundary; my responsibilities comprised data mining, manuscript design and writing.

Experimental work (%)	Supervision (%)	Manuscript (%)	Research direction (%)
50	100	80	90

[3] BABEK, Ondrej, **Tomas KUMPAN**, Jiri KALVODA and Tomas Matys GRYGAR. Devonian/Carboniferous boundary glacioeustatic fluctuations in a platform-to-basin direction: A geochemical approach of sequence stratigraphy in pelagic settings. *Sedimentary*

Geology [online]. 2016, **337**, 81–99. ISSN 1879-0968. Available at: doi:10.1016/j.sedgeo.2016.03.009
According to AIS GEOLOGY – SCIE Q1

Author's contribution to the publication: I participated in data collection, analysis and interpretation of detrital proxies, and contributed to publication design, synthesis and manuscript writing.

Experimental work (%)	Supervision (%)	Manuscript (%)	Research direction (%)
50	0	50	50

[4] HARTENFELS, Sven, Ralph Thomas BECKER, Hans-Georg HERBIG, Wenkun QIE, **Tomas KUMPAN**, David DE VLEESCHOUWER, Dieter WEYER and Jiri KALVODA. The Devonian-Carboniferous transition at Borkewehr near Wocklum (northern Rhenish Massif, Germany) - a potential GSSP section. *Palaeobiodiversity and Palaeoenvir*onments [online]. 2022, **102**(3), 763–829. ISSN 1867-1608. Available at: doi:10.1007/s12549-022-00531-5
According to AIS PALEONTOLOGY – SCIE Q3

Author's contribution to the publication: I contributed to this multidisciplinary paper (biostratigraphy, sedimentology, geochemistry, cyclostratigraphy) proposing a GSSP candidate, with responsibility for the design and writing of the element geochemistry section.

Experimental work (%)	Supervision (%)	Manuscript (%)	Research direction (%)
10	0	10	10

[5] KAISER, Sandra I., **Tomas KUMPAN** and Vojtech CIGLER. New unornamented siphonodellids (Conodonta) of the lower Tournaisian from the Rhenish Massif and Moravian Karst (Germany and Czech Republic). *Neues Jahrbuch fur Geologie und Palaontologie-Abhandlungen* [online]. 2017, **286**(1), 1–33. ISSN 0077-7749. Available at: doi:10.1127/njgpa/2017/0684
According to AIS PALEONTOLOGY – SCIE Q4

Author's contribution to the publication: I participated in the analysis of conodont material from the Moravian Karst, and was responsible for the development of the research and publication design and manuscript writing, with special focus on biostratigraphy and new species determination.

Experimental work (%)	Supervision (%)	Manuscript (%)	Research direction (%)
50	30	50	50

[6] ZHURAVLEV, V, Artem N. PLOTITSYN, Vojtech CIGLER and **Tomas KUMPAN**. Taxonomic notes on some advanced Tournaisian (Mississippian) siphonodellids (Conodonta). *Geobios* [online]. 2021, **64**, 93–101. ISSN 1777-5728. Available at: doi:10.1016/j.geobios.2020.12.001

According to AIS PALEONTOLOGY – SCIE Q2

Author's contribution to the publication: I participated in the analysis of conodont material from the Moravian Karst, and was responsible for the development of the research and manuscript writing, with special focus on biostratigraphy.

Experimental work (%)	Supervision (%)	Manuscript (%)	Research direction (%)
30	40	30	40

[7] CIGLER, Vojtech, **Tomas KUMPAN*(corresponding author)***, Jiri FRYDA, Jiri KALVODA and Stepan DAMBORSKY. Refinement of the lower Tournaisian (Mississippian) conodont, foraminiferal and carbon isotope stratigraphy of the Moravosilesian Basin (Czech Republic) and implications for global correlation. *Newsletters on Stratigraphy* [online]. 2025, **58**(1), 71–98. ISSN 0078-0421. Available at: doi:10.1127/nos/2024/0830

According to AIS GEOLOGY – SCIE Q1

Author's contribution to the publication: I designed and led the research, supervising my PhD student in conodont biostratigraphy and taxonomy, and was responsible for the analysis, interpretation and manuscript writing of the carbon isotope dataset.

Experimental work (%)	Supervision (%)	Manuscript (%)	Research direction (%)
50	100	60	90

[8] KALVODA, Jiri, **Tomas KUMPAN*(corresponding author)***, Marketa HOLA, Ondrej BABEK, Viktor KANICKY and Radek SKODA. Fine-scale LA-ICP-MS study of redox oscillations and REEY cycling during the latest Devonian Hangenberg Crisis (Moravian Karst, Czech Republic). *Palaeogeography Palaeoclimatology Palaeoecology* [online]. 2018, **493**, 30–43. ISSN 1872-616X. Available at: doi:10.1016/j.palaeo.2017.12.034

According to AIS PALEONTOLOGY – SCIE Q1

Author's contribution to the publication: As the corresponding author, I was responsible for coordinating the authors group, collecting, integrating and analysing results, and preparing the manuscript, with special focus on redox-sensitive trace elements.

Experimental work (%)	Supervision (%)	Manuscript (%)	Research direction (%)
60	40	50	60

[9] KUMPAN, Tomas*(corresponding author)*, Jiri KALVODA, Ondrej BABEK, Marketa HOLA and Viktor KANICKY. Tracing paleoredox conditions across the DCB event: A case study from carbonate-dominated settings of Belgium, the Czech Republic, and northern France. *Sedimentary Geology* [online]. 2019, **380**, 143–157. ISSN 1879-0968. Available at: doi:10.1016/j.sedgeo.2018.12.003
According to AIS GEOLOGY – SCIE Q1

Author's contribution to the publication: As the leading author, I designed the study, collected and analysed the dataset, and was responsible for manuscript preparation, including the formulation of conclusions and the overall structure of the text.

Experimental work (%)	Supervision (%)	Manuscript (%)	Research direction (%)
80	70	60	60

[10] KALVODA, Jiri, **Tomas KUMPAN*(corresponding author)***, Wenkun QIE, Jiri FRYDA and Ondrej BABEK. Mercury spikes at the DCB in the eastern part of the Rhenohercynian Zone (central Europe) and in the South China Block. *Palaeogeography Palaeoclimatology Palaeoecology* [online]. 2019, **531**(Article 109221). ISSN 1872-616X. Available at: doi:10.1016/j.palaeo.2019.05.043
According to AIS PALEONTOLOGY – SCIE Q1

Author's contribution to the publication: As the corresponding author, I coordinated the author group, integrated and analysed the results, and led manuscript preparation, with special focus on redox-sensitive trace elements.

Experimental work (%)	Supervision (%)	Manuscript (%)	Research direction (%)
70	60	40	60

[11] BABEK, Ondrej, Stanislava VODRAZKOVA, **Tomas KUMPAN**, Jiri KALVODA, Marketa HOLA and Lukas ACKERMAN. Geochemical record of the subsurface redox gradient in marine red beds: A case study from the Devonian Prague Basin, Czechia. *Sedimentology* [online]. 2021, **68**(7), 3523–3548. ISSN 1365-3091. Available at: doi:10.1111/sed.12910
According to AIS GEOLOGY – SCIE Q1

Author's contribution to the publication: I contributed to this multidisciplinary study (mineralogy, petrophysics, geochemistry) through *in situ* LA-ICP-MS microgeochemical data acquisition and interpretation, and participated in the synthesis and formulation of the study conclusions.

Experimental work (%)	Supervision (%)	Manuscript (%)	Research direction (%)
20	0	20	20

[12] BABEK, Ondrej, **Tomas KUMPAN**, Mikael CALNER, Daniel SIMICEK, Jiri FRYDA, Marketa HOLA, Lukas ACKERMAN and Katerina KOLKOVA. Redox geochemistry of the red `orthoceratite limestone' of Baltoscandia: Possible linkage to mid-Ordovician palaeoceanographic changes. *Sedimentary Geology* [online]. 2021, **420**(Article 105934). ISSN 1879-0968. Available at: doi:10.1016/j.sedgeo.2021.105934

According to AIS GEOLOGY – SCIE Q1

Author's contribution to the publication: My role in this multidisciplinary study (mineralogy, petrophysics, geochemistry) centred on *in situ* LA-ICP-MS microgeochemistry, encompassing data acquisition, interpretation, and contribution to the synthesis and conclusions.

Experimental work (%)	Supervision (%)	Manuscript (%)	Research direction (%)
30	0	30	30

[13] BABEK, Ondrej, **Tomas KUMPAN**, Wenjie LI, Marketa HOLA, Daniel SIMICEK and Jaroslav KAPUSTA. Incipient reddening of Ordovician carbonates: The origin and geochemistry of yellow and pink colouration in limestones. *Sedimentary Geology* [online]. 2022, **440**(Article 106262). ISSN 1879-0968. Available at: doi:10.1016/j.sedgeo.2022.106262

According to AIS GEOLOGY – SCIE Q1

Author's contribution to the publication: In this multidisciplinary study (mineralogy, petrophysics, geochemistry), I provided *in situ* LA-ICP-MS microgeochemical data and the corresponding manuscript sections, contributing to the geochemical interpretation and overall synthesis of the conclusions.

Experimental work (%)	Supervision (%)	Manuscript (%)	Research direction (%)
30	0	30	30

Author's contribution to the publication: I participated in this multidisciplinary study (mineralogy, petrophysics, geochemistry) by contribution of data and manuscript parts from *in situ* LA-ICP-MS microgeochemistry, providing intrepretation and synthesis for the study conclusions.

[14] BABEK, Ondrej, **Tomas KUMPAN**, Stanislava VODRAZKOVA and Catherine GIRARD. Fluctuating seafloor oxygenation before, during and after the Frasnian/Famennian crisis: Quantitative colour analysis and geochemistry of Upper Devonian marine red beds, Montagne Noire, S. France. *Facies* [online]. 2026, **72**(1, Article 7). ISSN 1612-4820. Available at: doi:10.1007/s10347-025-00719-z

According to AIS GEOLOGY – SCIE Q1

Author's contribution to the publication: I was responsible for the *in situ* LA-ICP-MS microgeochemical component of this multidisciplinary study (mineralogy, petrophysics,

geochemistry), contributing data, manuscript sections, and geochemical interpretation to the overall synthesis and conclusions.

Experimental work (%)	Supervision (%)	Manuscript (%)	Research direction (%)
30	0	30	30

[15] VODRAZKOVA, Stanislava, **Tomas KUMPAN**, Radek VODRAZKA, Jiri FRYDA, Renata COPJAKOVA, Magdalena KOUBOVA, Axel MUNNECKE, Jiri KALVODA and Marketa HOLA. Ferruginous coated grains of microbial origin from the Lower Devonian (Pragian) of the Prague Basin (Czech Republic) - Petrological and geochemical perspective. *Sedimentary Geol*ogy [online]. 2022, **438**(Article 106194). ISSN 1879-0968. Available at: doi:10.1016/j.sedgeo.2022.106194

According to AIS GEOLOGY – SCIE Q1

Author's contribution to the publication: My contribution to this multidisciplinary study (mineralogy, petrology, geochemistry) comprised *in situ* LA-ICP-MS microgeochemical data acquisition, interpretation, and synthesis, with direct input into the formulation of the study conclusions.

Experimental work (%)	Supervision (%)	Manuscript (%)	Research direction (%)
30	0	40	40

2 Advances in Devonian and Carboniferous Stratigraphy

The Devonian and Carboniferous periods represented a critical transition in history of the Earth, witnessing fundamental changes in marine and terrestrial ecosystems, paleogeography and paleoclimate (Aretz et al. 2020; Becker et al. 2020). Both were one of the first defined stratigraphic systems (Conybeare and Phillips 1822; Murchison and Sedgwick 1839), with pioneering work establishing regional chronostratigraphic frameworks that continue to evolve today (Gradstein et al. 2020).

The development of stratigraphy, particularly introduction of conodont biostratigraphy in the mid-20th century revolutionized correlation capabilities for these systems, providing high-resolution zonation schemes that enabled precise intercontinental correlations previously impossible with macrofossils alone (Branson and Mehl 1930; Voges 1959; Ziegler 1971). From the 1970s, research focus increasingly shifted toward chronostratigraphic boundaries and global events (Walliser 1984), and defining and refining the geological timescale through the Global Boundary Stratotype Section and Point (GSSP) concept (Chlupáč et al. 1972; Cowie et al. 1986). Later, chemostratigraphic techniques, particularly carbon isotope stratigraphy, has emerged as a powerful complement to traditional biostratigraphy, enabling higher-resolution integrated stratigraphic correlation and subdivision (Saltzman 2002; Buggish et al. 2008; Saltzman and Thomas 2012).

My research addresses several key stratigraphic challenges of the Upper Devonian and lower Carboniferous, focusing primarily on Devonian–Carboniferous Boundary redefinition and the refinement of lower Carboniferous (Tournaisian) correlation schemes. In **Topic A**, I addressed both the problematic nature of the current GSSP and potential solutions involving conodont biostratigraphy (**Paper 1**) and elemental chemostratigraphy (**Papers 2 and 3**). The following **Topic B** provides commentary on advances in lower Tournaisian stratigraphy, including refined conodont taxonomy and biostratigraphy (**Papers 4 to 6**) and carbon isotope chemostratigraphy (**Paper 7**).

2.1 Topic A: Redefinition of the Devonian-Carboniferous System Boundary

The Devonian-Carboniferous Boundary (DCB; Fig. 2) was the first chronostratigraphic level to be formally defined internationally, initially placed at the first appearance of the goniatite *Gattendorfia subinvoluta* (Jongmans 1938). Strong biogeographic provincialism rendered global correlations impractical, and subsequent conodont biostratigraphic studies revealed a stratigraphic gap at the chosen boundary level in the

stratotype Ober-Röddinghausen in Rhenish Massif (Alberti et al. 1974), necessitating a search for a new boundary definition. This led to the establishment of an International Working Group on the DCB in 1976. After 15 years of intensive research and controversial discussions (Ziegler and Sandberg 1996), a new Global Standard Section and Point (GSSP) was placed at the base of Bed 89 in La Serre E' trench in the Montagne Noire, marked by the first appearance of conodont *Siphonodella sulcata* HUDDLE in the lineage from ancestor *Si. praesulcata* SANDBERG (Flajs and Feist 1988; Paproth et al. 1991). However, subsequent work at La Serre confirmed that the same siphonodellid morphotype used to place the GSSP occurs in a lower Bed 84 (Kaiser 2009). Moreover, GSSP golden spike is situated within an oolitic limestone with significant reworking of conodonts (Ziegler and Sandberg 1996). The definition of the GSSP elsewhere is further complicated by the lack of stratigraphically continuous, non-condensed successions across the boundary in global perspective.

Hangenberg Crisis

The lack of continuous and lithologically monotonous DCB successions suitable for GSSP is result of stratigraphic gaps or event facies related to the Hangenberg Biocrisis or Crisis (Fig. 2). I prefer the term "Crisis" over "Biocrisis" in thesis, as the event encompassed changes extending beyond the biotic realm. This was a major geochemical, climatic and ecological turnover resulting in the extinction of Famennian ecosystems and significantly impacting both terrestrial and marine palaeobiodiversity and ecology (for details see Kaiser et al. 2015).

The Hangenberg Crisis was a cascade of events, which subdivision is based on the lithostratigraphy in the event type area, Rhenish Massif ("Standard Rhenish Succession", Fig. 1; Becker et al. 2016). The preludium interval (Drewer Sandstone Event; *praesulcata* conodont Zone sensu Kaiser et al. 2009; this zonation is used herein for the Famennian) is not often well recognized out of Rhenish Massif, but the **lower crisis interval** (Hangenberg Black Shale Event; *costatus-kockeli* conodont Interregnum) marks the carbonate crisis (**Paper 3**) and main extinction event in the marine realm of global extent (Kaiser et al. 2015). The **middle crisis interval** (Hangenberg Sandstone Event, *costatus-kockeli* condont Interregnum) is manifested by deposition of relatively coarser-grained siliciclastics or stratigraphic gaps (Kaiser et al. 2015; **Papers 2 to 4**). The **upper crisis interval** (Stockum Limestone Event; *kockeli* conodont Zone) saw the restoration of carbonate productivity and the evolutionary radiation of numerous groups of organisms (Kaiser et al. 2015; Becker et al. 2016).

Testing the solutions for revised DCB

Due to the problems related to the current GSSP, the "Devonian-Carboniferous GSSP Reappraisal Task Group" was established under the International Commission on Stratigraphy in 2009, gathered from members of the Subcommission on Devonian

Stratigraphy and Subcommission on Carboniferous Stratigraphy (Aretz and Corradini 2021). I have had the honour of serving as a voting member of the Reappraisal Task Group since 2021 (corresponding member since 2015). In the past years, task group members put effort into searching for new criteria for the new boundary definition, both from the point of view of biostratigraphy, sequence stratigraphy, event stratigraphy and chemostratigraphy (e.g. Corradini et al. 2011; Kaiser and Corradini 2011; **Kumpan et al. 2014a, 2014b, 2015**; Becker et al. 2016). Consequently, several options were critically evaluated during the workshop in Montpellier 2016, leading to selection of the "Montpellier Criteria" for new DCB definition (Aretz and Corradini 2019). The criteria were subsequently ratified by 60% of voting members during task group meeting at International Congress on the Carboniferous and Permian, Cologne 2019 (Aretz and Corradini 2021).

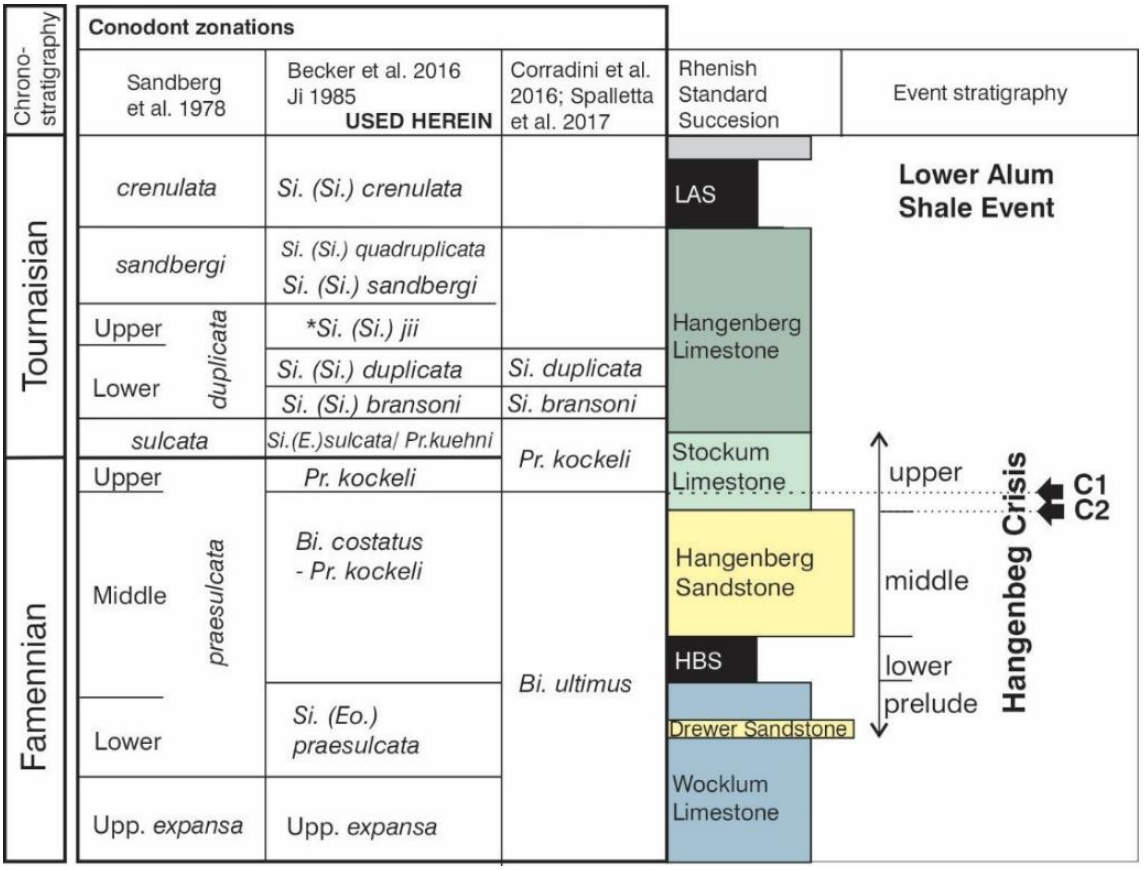

Figure 2. Conodont zonations and event stratigraphic framework of Devonian-Carboniferous interval and Hangenberg Crisis. Arrows marks positions of two proposed levels in the time line of Montepellier Criteria (C1 - base of the *Protognathodus kockeli* conodont Zone; C2 - end of the maximum regression). Abbreviatons: HBS – Hangenberg Black Shale, LAS – Lower Alum Shale).

The proposed boundary level is defined by four criteria applied as a multicriteria "time-line" approach: (1) the base of the *Protognathodus kockeli* conodont Zone, (2) the end of the Devonian mass extinction, (3) the beginning of the Carboniferous radiation, and (4) the top of a major regression (Aretz and Corradini 2021). This multicriteria approach aims to reduce dependence on a single marker and increase the potential for placing the boundary in different facies realms and palaeobiogeographical provinces. In the following years until now, the criteria are being tested globally before GSSP sections will be selected for the final proposal in 2028.

2.1.1 Testing conodont biostratigraphy solution for DCB

As the base of the *Protognathodus kockeli* conodont Zone is considered as a principal potential criterion for redefining the DCB, and first occurrence of *Protognathodus kockeli* is primary zonal marker, I studied taxonomy and biostratigraphy of protognathodids across DCB at two classical peri-Gondwanan sections in Carnic Alps and Graz Paleozoic (Fig. 1) to test the application of this criterion (**Paper 1**). The question was whether this zone can be placed with sufficient stratigraphic precision and reproducibility to serve as a GSSP marker. The choice of studied sections - Grüne Schneid in the Carnic Alps (Schönlaub et al. 1988, 1992; Kaiser et al. 2006, 2008, 2009; Corradini et al. 2017) and Trolp in the Graz Paleozoic (Nössing 1975; Ebner 1978; Kaiser et al. 2009) - was determined by the need for hemipelagic limestone successions with minimal siliciclastic interruption and stratigraphic gaps in the Hangenberg Crisis interval. A conodont record through the crisis interval requires limestone-dominated successions, as conodonts are absent from shales and sandstones of the crisis facies. Their absence obliterates the biostratigraphic record and introduce preservational bias affecting first and last occurrences. On the other hand, disadvantage of this setting is stratigraphic condensation around the DCB, which leads to bias during high-resolution sampling (**Paper 1**).

The protognathodid lineage comprises a sequence of morphological changes from *Protognathodus collinsoni* ZIEGLER, through transitional forms to *Pr. kockeli* (BISCHOFF) and *Pr. kuehni* (ZIEGLER & LEUTERITZ), with the key discriminating criterion being the arrangement of nodes and platform symmetry. *Protognathodus collinsoni* bears scattered nodes, whereas at least one linear row of nodes (minimum three) characterises *Pr. kockeli* (sensu Corradini et al. 2011), and transverse ridges define *Pr. kuehni* (Corradini et al. 2011). However, the transition between *Protognathodus collinsoni* and *Pr. kockeli* involves intermediate forms (Fig. 3a), and the discrimination between „single scattered nodes" as a feature of *Pr. collinsoni* and early "one-row" arrangements characteristic of *Pr. kockeli* (Fig. 3b) are difficult to apply consistently. In the studied material, "one-row" and "two-rows" morphotypes were distinguished (Fig. 3c). *Protognathodus kockeli* elements with more rows on each side of platform are considered as advanced morphotypes (Fig. 3D), and some aberrant forms occur as well.

At both sections, *Protognathodus kockeli* enters above the main biofacies change of the Hangenberg Crisis interval, although the precise stratigraphic position of its first occurrence relative to the crisis beds remains uncertain due to condensation and potential faunal mixing. At Trolp, the "one-row" morphotype precedes the "two-row morphotype", whereas at Grüne Schneid the stratigraphic relationship between the two morphotypes is probably obscured by condensed boundary interval, which can lead to mixing in samples taken from subdivided thin nodular limestone bed (**Paper 1**).

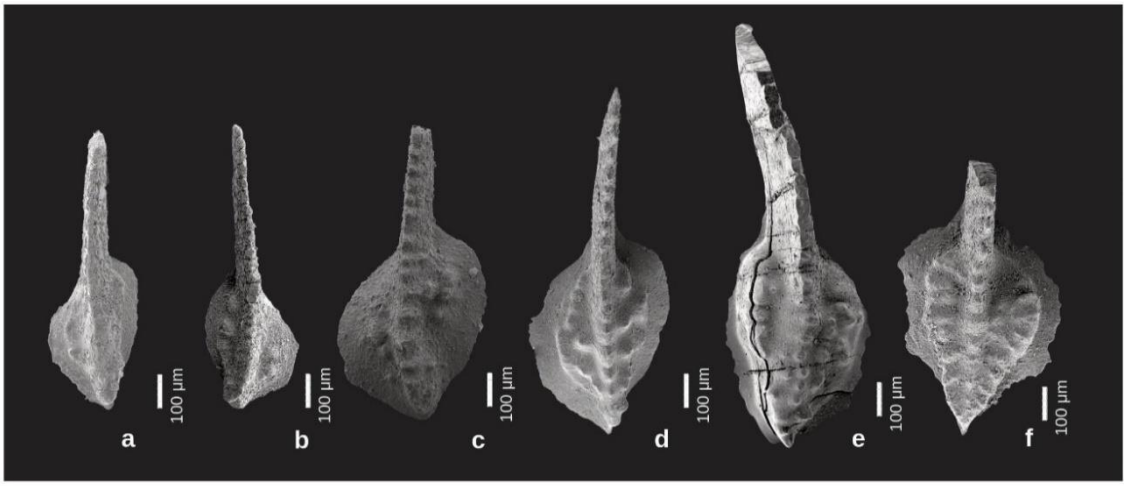

Figure 3. Examples of elements from the evolutionary lineage *Protognathodus collinsoni – Pr. kockeli – Pr. kuehni* from the Grüne Schneid section, Carnic Alps. (**a**) 7. *Protognathodus collinsoni-kockeli*, Bed 6b1; (**2**) *Protognathodus kockeli*, "one-row" morphotype, (**c**) Bed 6b2; *Protognathodus kockeli*, "two-rows" morphotype, Bed 6b; (**d**) *Protognathodus kockeli*, advanced form, more than two rows of nodes, Bed 6c; (**e**) *Protognathodus kockeli-kuehni*, Bed 6c1; (**f**) *Protognathodus kuehni*, Bed 6c2.

From the perspective of the ongoing GSSP reappraisal, **paper 1** concluded that the taxonomic complexity of the *Protognathodus collinsoni–Pr. kockeli* lineage pose obstacle to its use as the criterion. A taxonomic re-evaluation of the early protognathodids was identified in the **paper 1** as a necessary precondition before a distinctive conodont-based DCB definition could be settled. Subsequently, Hartenfels et al. (2022; **paper 4**, in which I contributed elemental geochemistry only) formally addressed part of this problem by establishing the new species *Protognathodus semikockeli* HARTNEFELS ET AL., the previous "one-row" morphotype, which has first occurrence in the first limestone above Hangenberg Crisis clastic interval (Stockum Limestone Event) in Rhenish Massif (Borkewehr) and Montagne Noire (Puech de la Suque). The establishment of *Protognatodus semikockeli* narrowed the concept of *Pr. kockeli* to elements bearing at least one row of nodes along both margins of the platform (previous "two rows morphotypes). *Protognathodus kockeli* enters above *Pr. semikockeli* within the Stockum Limestone Event at Borkewehr in Rhenish Massif, Puech de la Suque in Montagne Noire (**Paper 4**), and Trolp in Graz Paleozoic (**Paper 1).**

However, *Protognathodus semikockeli-Pr. kockeli* lineage was not been documented beyond these three areas, representing records of Laurussian and peri-Gondwanan basins. The geographic distribution of *Protognathodus* across the DCB is heterogeneous and largely controlled by facies and preservational bias rather than true biogeographic restriction (Corradini et al. 2011). The results of **papers 1 and 4** support the view that regions with pelagic to hemipelagic limestone successions, Montagne Noire, Carnic Alps, and Graz Palaeozoic, often document a complete evolutionary succession. On the other hand, other areas, including e.g., the Moravian Karst (**Paper 2**), Pyrenees, Thuringia, South China, and the Subpolar Urals, yield only partial records (Hartenfels et al. 2022). This is partly a result of the shift from carbonate to clastic deposition unfavourable for conodont preservation, and partly of the absence of detailed taxonomic revision of the *Protognathodus semikockeli-Pr. kockeli* fauna. Nevertheless, the first occurrence of *Protognathodus kockeli* in its emended definition (Hartenfels et al. 2022), combined with the independent criterion of the "top of a major regression" documented in the following section, provides a basis for a multicriteria boundary approach.

2.1.2 Testing Element Chemostratigraphy for DCB

The Hangenberg Crisis left a distinct lithological and geochemical signature in marine sediments: common stratigraphic gaps, sharp facies changes, cessation of carbonate deposition and shift to siliciclastics, fossil-free horizons (Kaiser et al. 2015; Becker et al. 2016). These changes provide highly distinctive surfaces, well traceable both lithologically and geochemically, and some of these surfaces were proposed as having chronostratigraphic application, represented in the fourth Montpellier criterion.

To test the applicability of the criterion "top of a major regression (of the Hangenberg Crisis)" (Fig. 2), concentrations of lithophile elements hosted predominantly in detrital siliciclastic grains were selected as proxies for clastic input into carbonate marine environments related with sea-level fall. The most commonly used detrital proxies Al, Ti, Th, and Zr are abundant in crustal rocks and relatively immobile during weathering, transport, and diagenesis (McLennan 2001). Stratigraphic variations in their concentrations and ratios thus reflect clastic input quantity and grain size, and by extension sea-level changes and weathering intensity, which can be traced also in monotonous fine-grained sediments without facies changes (Sageman and Lyons 2005; Craigie 2018).

Data gathered and published during my doctoral study (Kumpan et al. 2014a, 2014b, 2015) and subsequent research (**papers 2 to 4; Kumpan et al. 2018)** provided a high-resolution chemostratigraphic framework for the DCB across Central, Southern and Western Europe, and North America (Fig. 1). Element composition of bulk samples for these studied were analysed from powdered samples using Energy Dispersive X-ray Fluorescence (EDXRF) spectrometers MiniPal 4.0 (PANalytical; Institute of

Inorganic Chemistry of Czech Academy of Sciences; details on method in the **papers 2 to 4**). I was responsible for research and sampling design, geochemical data interpretation and chemostratigraphic correlation across studied sections.

In general, the geochemical record reveals a sudden change in detrital supply at the base of the lower phase of Hangenberg Crisis (Fig. 4). It is commonly marked by abrupt increases in Al, K, Rb and Zr above the last occurrence of the *Siphonodella praesulcata* conodont fauna, accompanied by significant decreases in Ca concentrations and K/Al ratios, both in completely carbonate succession or related with shift in lithology (limestone to marlstone/shale). In most of the sections, lithological and geochemical data indicate a shutdown or strong limitation of carbonate productivity (carbonate crisis), usually manifested by black or grey shale, but the response varied between depositional settings. In some setting the carbonate deposition persisted during the crisis (**Papers 3 and 4**). Nearshore carbonate productivity continued during the Hangenberg Crisis in the homoclinal ramp settings of the Namur-Dinant Basin (**Kumpan et al. 2014b**; **Paper 3**). In marine slope settings of the Moravian Karst, the lower phase of the crisis (Hangenberg Black Shale Event) was recorded as microbial-authigenic limestone (**Paper 2 and 8**). The monotonous hemipelagic successions with prevailing limestone deposition show strong condensation, as illustrated in **papers 1 and 3**.

In deposits of the middle crisis phase (Hangenberg Sandstone Event), progradation from finer-grained lower phase deposits into coarser-grained sediments is reflected in distinct Zr/Al (or Zr/Rb, where Al was bellow detection limits and Rb was used for normalisation instead; **Paper 3**) patterns. This geochemical signature is traceable across depositional environments from neritic to hemipelagic settings of Laurussian and peri-Gondwanan basins, providing a robust interregional correlation tool (Fig. 4). The sharp increase or peak of Zr/Al both in monotonous hemipelagic succession and lithologically more diverse neritic sections were interpreted as a record of coarsening of clastic material (**Paper 2** and **3**). This coarsening was driven by glacioeustatic sea-level fall resulting in forced regression and stronger continental runoff, is well supported by direct evidence of latest Devonian Gondwana glaciation (Isaacson et al. 2008; Lakin et al. 2016). The significantly elevated terrigenous Al_2O_3 accumulation rates across all depositional settings, including the most distal pelagic ones (**Paper 3**), confirm that the Zr/Al increase records genuine enhancement of continental flux rather than sediment starvation, supporting a top-down (Carmichael et al. 2016) nutrient supply model for Hangenberg anoxia.

The geochemical record of maximum clastic input, coinciding with the top of the middle crisis regressive pulse, can be traced as a near-synchronous stratigraphic surface consistently preceding the *Protognathodus kockeli* Zone (Fig. 4). This relationship was documented across a range of settings in Laurussian basins by my research: in the Rhenish Massif at the candidate GSSP section Borkewehr, where the Zr/Al peak marks the top of the regression within the Hangenberg Shale and Sandstone unit (Kumpan et al. 2015; **Papers 3 and 4**); in the Moravian Karst, where the Zr/Al peak lies just below

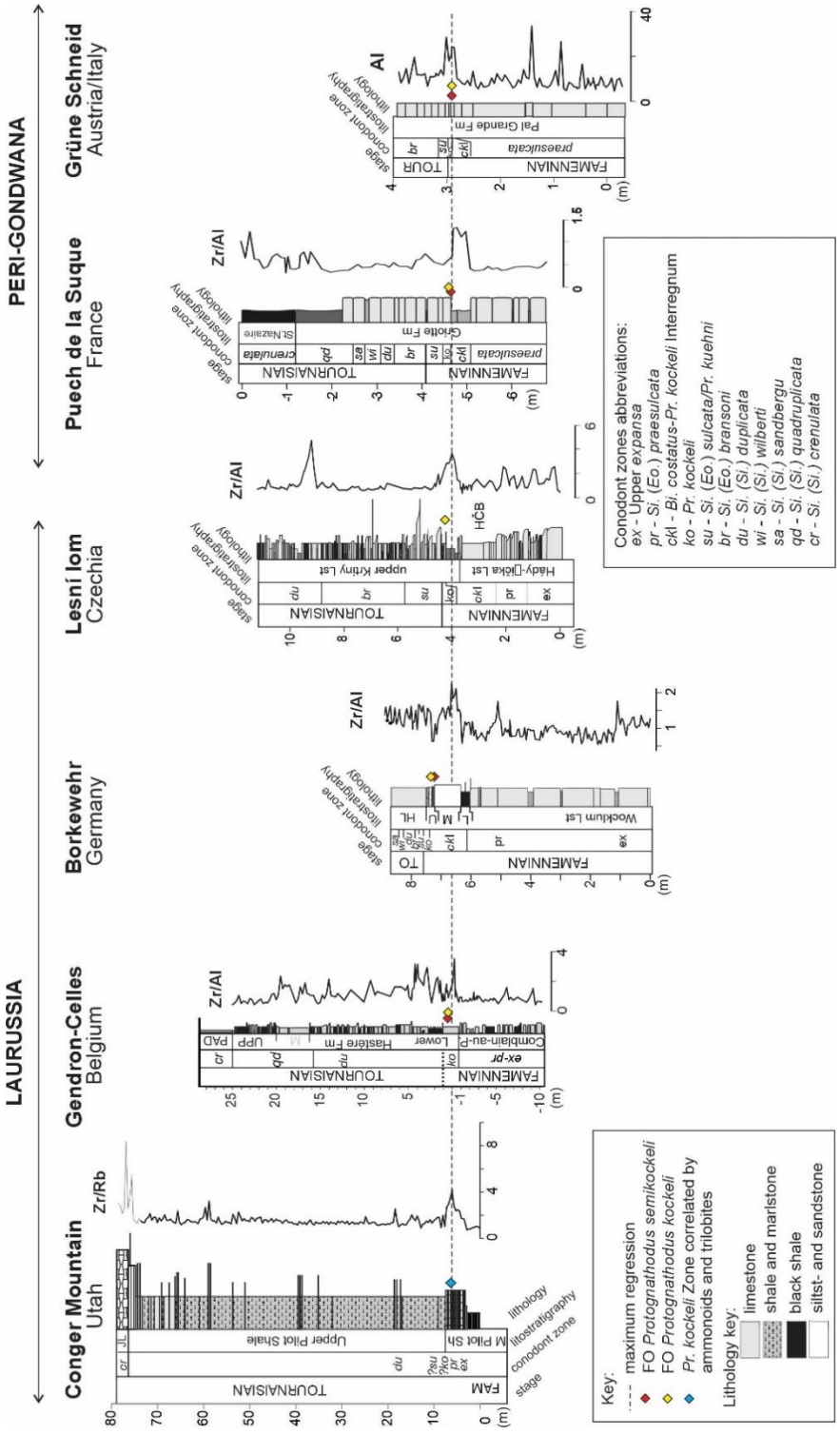

Figure 4. Reference Devonian-Carboniferous sections for studied Laurussian and peri-Gondwanan basins. The Zr/Al (or Zr/Rb and Al; see text for explanation) curves are based on data obtained by EDXRF analysis. The main correlation surface is the Zr/Al (Zr/Rb) peak below the first occurrence of *Protognathodus kockeli*.

the limestone nodules bearing the first *Protognathodus. kockeli*, both in carbonate turbidites of lower slope setting and in hemipelagites of the upper slope setting (**Paper 2**; Malá 2020); in the neritic facies of the Namur-Dinant Basin, where the Zr/Al peak was identified in the basal regressive bed of the Hastière Formation, with the FO of *Protognathodus kockeli* reported from the bed above (Bouckaert and Groessens 1976; Conil et al., 1986; Denayer et al. 2021; **Paper 2 and 9**).

The same situation was documented in peri-Gondwanan basins: peak in Zr/Al occur just below the *Protognathodus kockeli* Zone at Puech de la Suque in Montagne Noire (Fig. 4). In condensed pelagic sections such as Grüne Schneid in Carnic Alps, the FO of *Protognathodus kockeli* takes place within the interval with increased detrital content marked by Al peak, as result of stratigraphic condensation (Kumpan et al. 2014a; **Paper 1**). However, even under condensed conditions, the detrital peak consistently precedes or coincides with the FO of *Protognathodus kockeli*, never occurring above it.

The boundary in protognathodid-free DCB succession

A representative example of the application of the "end of maximum regression" criterion in sections lacking protognathodids are DCB successions in Utah, USA at the boundary between the Middle and Upper Pilot Shales (Sandberg and Poole 1977; Sandberg et al. 1980; Cole et al. 2015; *Kumpan in prep*.). The Zr/Rb peak was detected within the upper part of the Middle Pilot Shale, the oncolitic Leatham Member (Fig. 4; sections Conger Mountain, Little Mile-and-a-Half Canyon, Burbank Hills; **Kumpan et al. 2018**). However, the biostratigraphy of the Leatham Member and overlying Upper Pilot Shale remains controversial, and no consensus exists regarding the precise position of conodont zonal boundaries at DCB in these successions. According to conodont data, the oncolitic interval of the Leatham Member corresponds broadly to the Late *expansa–praesulcata* interval, whereas the overlying Upper Pilot Shale has yielded faunas ranging from the *Siphonodella sulcata* to *Si. duplicata* zones (Sandberg et al. 1980; although the older age, e.g. *kockeli* Zone for the lower part of the Upper Pilot Shale could not be excluded, Cole et al. 2015; Sandberg, personal communication). Importantly, the uppermost part of the Leatham Member above the Zr/Rb peak falls within an unzoned interval lacking diagnostic conodont faunas, as well as lower part of the Upper Pilot Shale (Sandberg and Poole 1977). Alternatively, assignment of the oncolitic member to the *Protognathodus kockeli* Zone was based on indirect evidence from trilobites (Feist and Petersen 1995) and goniatites (*Acutimitoceras*; T. R. Becker, personal communication).

Based on the evidence presented above, the oncolitic Leatham Member can be interpreted as regressive intercalation within an otherwise deep-water shale succession developed in response to the Hangenberg maximum regression. The Zr/Rb peak recorded within this interval coincides with a macrofossil assemblage potentially indicative of the *Protognathodus kockeli* Zone in the unzoned interval. The end-of-maximum-

regression criterion can therefore be reliably applied at the oncolitic Leatham Member in conjunction with auxiliary biostratigraphic data. The DCB would thus be placed immediately above the Zr/Rb peak, marking the transition from the regressive oncolitic facies to the renewed deepening recorded in the lower Upper Pilot Shale.

2.1.3 Conclusive remarks

My research summarized in **Topic A** demonstrates that the two Montpellier Criteria (base of the *Protognathodus kockeli* conodont Zone and lavel above maximum regression) are applicable across a wide range of depositional settings, consistently showing the top of the major regression and the base of the *Protognathodus kockeli* Zone as successive events (Fig. 4). The Zr/Al or other peaks of detrital geochemical proxies representing maximum regression provide a correlative surface traceable across contrasting depositional environments, while the conodont lineage provides the biological time anchor. However, "one-row"-"two-rows" *Protognathodus kockeli,* or *Pr. semikockeli - Pr. kockeli* lineage documentation is geographically limited to Rhenish Massive, Carnic Alps and Montagne Noire (**Papers 1 and 4**). Future application of the criterion should adopt the emended diagnosis of *Protognathodus kockeli* restricted to forms bearing at least two rows of nodes (Hartenfels et al. 2022), which provides a more precise and reproducible morphological definition for boundary placement.

Neither criterion is universally applicable for random sections, where *Protognathodus kockeli* is absent, and the geochemical surface alone cannot place the boundary with chronostratigraphic precision without biostratigraphic calibration from a reference section, which was demonstrated in Utah sections (Fig. 4). Nevertheless, their combination resolves the principal weaknesses of the current GSSP definition.

2.2 Topic B: Advances in lower Tournaisian stratigraphy

The early Tournaisian was a time of evolutionary radiation when late Palaeozoic ecosystems began to develop in the aftermath of the Hangenberg Crisis (Yao et al. 2020). Currently, the Tournaisian stage is not formally subdivided, but an informal three-fold division is traditionally applied in pelagic facies realms (Aretz et al. 2020); the lower Tournaisian corresponds to the strata between the DCB and the base of the Lower Alum Shale Event (base of the *Siphonodella crenulata* Zone, Fig. 2; Becker 1993). The early Tournaisian recovery after Hangenberg Crisis was marked by complex feedbacks between biotic evolution and environmental perturbations (carbon cycle perturbations, redox fluctuations, climatic shifts), whose exact triggers and causal mechanisms remain a matter of ongoing research (Yao et al. 2015; Liu et al. 2019; Qie et al. 2023). High-resolution stratigraphic frameworks are therefore essential for tracing evolutionary pathways and palaeoenvironmental changes in this interval. My contribution to the field was early Tournaisian conodont taxonomy and biostratigraphy (**Papers 5-**

7) combined with carbon isotope chemostratigraphy (**Papers 7**), leading to improvement for interregional correlation. The Moravian Karst area provided unique material for such study: conodont- and foraminifer-bearing limestones exposed in comparatively large thicknesses (4–20 m; **Paper 7**), in contrast to the condensed lower Tournaisian successions of many other regions (Carnic Alps, Graz Palaeozoic, Montagne Noire; ~1 m; e.g., **Paper 3; Kumpan et al. 2015; Feist et al. 2021; Spalletta et al. 2021**).

Chrono-stratigraphy		Event-stratigraphy	„cosmopolitan"			east Europe and Ural		China
			Sandberg et al. 1978	Ji 1985 Kaiser et al. 2009	**Zhuravlev et al. 2021**	Kulagina et al. 2013	Zhuravlev Plotitsyn 2022	Qie et al. 2021
MT		LAS	L *crenulata*	*crenulata*	*Si. crenulata*	*crenulata*	*Si. crenulata*	*Si. eurylobata*
lower Tournaisian	Hastarian		*sandbergi*	*quadruplicata*	*Si. quadruplicata*	*quadruplicata*	*Si. ludmilae*	*Si. sinensis*
				sandbergi	*Si. sandbergi*	*belkai*		
			U *duplicata*	*hassi*	*Si. wilberti*			*Si. homo-simplex*
			L *duplicata*	*duplicata*	*Si. duplicata*	*duplicata*		
				bransoni	*Si. bransoni*			
		HC	*sulcata*	*sulcata/ kuehni*	*Si. sulcata*	U L *sulcata*	*Si. semichato.*	*Po. spicatus*

Figure 5. Conodont zonation schemes of the lower-middle Tournaisian. Red colour highlights the revised zonation and correlation based on the results of my research (**Papers 5** and **6**). Abbreviations: MT – middle Tournaisian; HC – Hangenberg Crisis, LAS – Lower Alum Shale Event.

2.2.1 Revised lower Tournaisian conodont taxonomy and biostratigraphy

The early-middle Tournaisian was characterised by rapid evolution of the genus *Siphonodella*, providing a high-resolution biostratigraphic tool (Sandberg et al. 1978; Becker et al. 2016, 2021, **Papers 7 and 6**). Although the *Siphonodella*-based zonation has proven useful in the lower Tournaisian, biozonations vary between different paleogeographic regions and facies, and separate schemes were developed for open-marine and neritic deposits or paleogeographic areas (Fig. 5; Ji and Ziegler 1992; Zhuravlev 2007; Qie et al. 2014, 2016). An unresolved issue is restricted paleogeographic distribution of unornamented or less ornamented forms known from the East European Platform and Ural Mountains ("eastern European siphonodellid" group) and its correlation with the zonations based on "cosmopolitan" normally-ornamented siphonodellids, widely used in North Amerika, Western, Central and Southern Europe. I have addressed this gap in the **papers 5 to 7** by study of conodont material from the Moravian Karst, Montagne Noire, Rhenish Massif (Fig. 1) and North and Cis-Urals, including new material and figured specimens from previous publications. I was responsible for data collecting, taxonomic revision, definition of new species, biostratigraphic interpretation, and for the synthesis of regional correlation schemes.

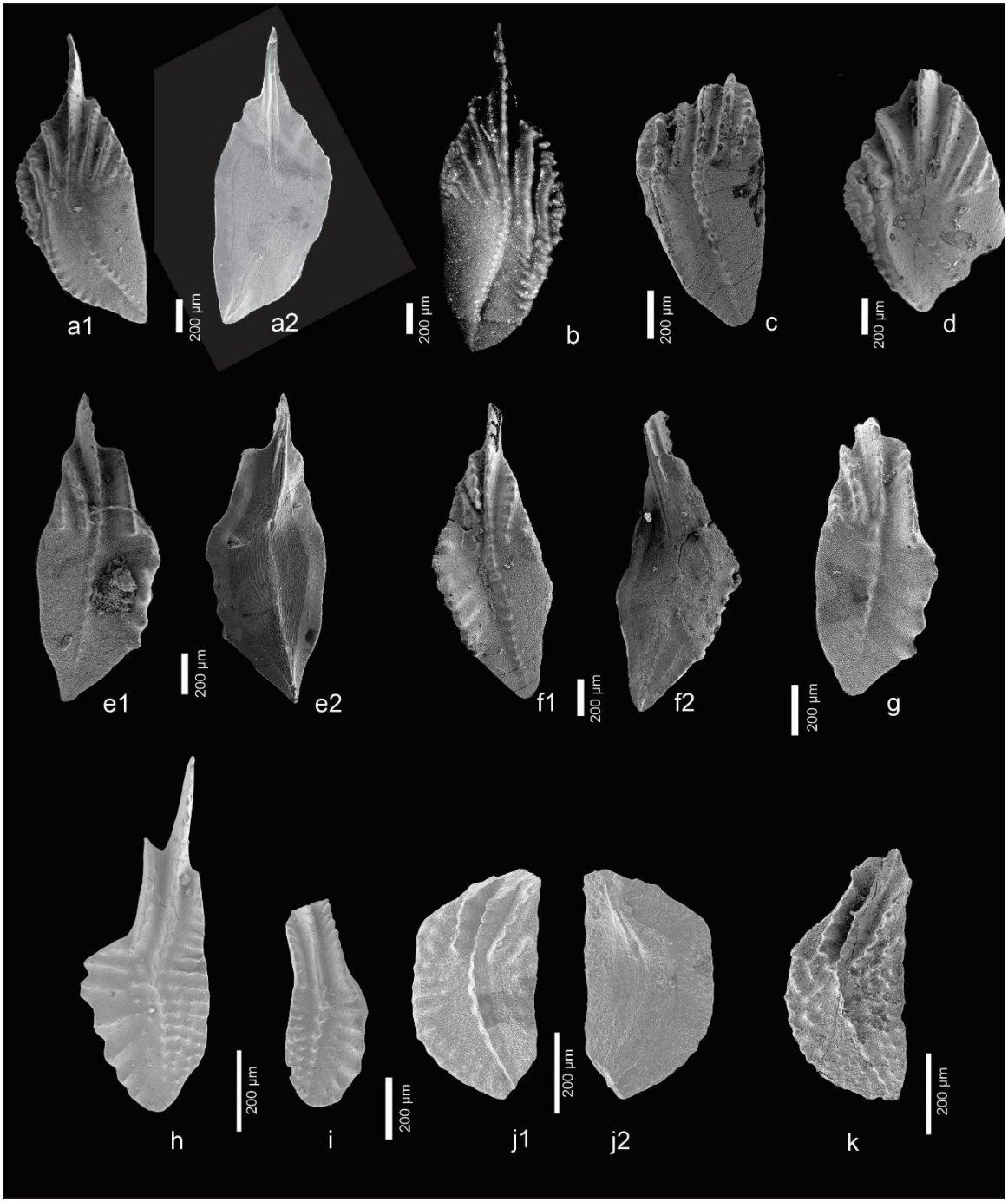

Figure 6. Representatives of unornamented "east European" representatives of the genus *Siphonodella* from the Moravian Karst, Lesní lom quarry: (**a**) *Siphonodella belkai* M1, bed CA4-1, *wilberti* Zone; (**b**) *Si. belkai* M2, CA4-1, *wilberti* Zone; (**c**) *Si. belkai* M1, bed CA2-760; base of the *wilberti* Zone; (**d**) *Si. belkai* M1, bed CA4-1, *wilberti* Zone; (**e**) *Si. kalvodai*, holotype, bed CA4-1, *wilberti* Zone; (**f**) *Si. kalvodai*, bed CA4-1, *wilberti* Zone; (**g**) (**e**) *Si. kalvodai*, bed VC7, *wilberti* Zone; (**h**) *Siphonodella* sp. A, bed LL2 35, *sandbergi* Zone; (**i**) *Siphonodella* sp. A, bed LL2 35, *sandbergi* Zone; (**j**) *Si. leiosa*, bed CA2-760, *Si. wilberti* Zone; (**k**) *Si.* cf. *leiosa*, bed LL2 35, *sandbergi* Zone.

Unornamented "east European siphonodellid" species were discovered in the Moravian Karst and Rhenish Massif, areas where they were previously unknown (**Papers 5 and 7**). This reveals a wider paleogeographic distribution of the group than previously recognised. The most common is *Siphonodella belkai* DZIK (Fig. 6a-d; **Paper 5**), while very rare are *Siphonodella leiosa* SOUQUET, CORRADINI & GIRARD (Fig. 6j-k), and newly described species *Siphonodella kalvodai* KAISER, KUMPAN & CIGLER and *Siphonodella* sp. A (Fig. 6f-h; **Paper 7**). These results suggest migration of the eastern European group into the eastern Laurussian margin from eastern Paleotethys regions. Their absence in western Laurussia was possibly impeded by forming Variscan and Acadian collision zones (**Paper 5**).

Several longstanding taxonomic issues concerning the stratigraphically and evolutionarily important species *Siphonodella wilberti* BARDASHEVA, BARDASHEV, WEDDIGE & ZIEGLER were resolved (**Paper 6**). This species was previously known under the names *Siphonodella duplicata sensu* Hass (Hass 1959), *Si. hassi* JI, and *Si. jii* (JI) (Becker et al. 2016). The taxonomic analysis in **paper 6** synonymised all these names with *Siphonodella wilberti* (Bardasheva et al. 2004) and identified it as the only available valid name. The revised taxonomy stabilises the definition of the *Siphonodella wilberti* Zone (Fig. 5; previously *Si. hassi* Zone or *Si.* (*Eo.) jii* Zone; Ji 1985, Kaiser et al. 2019) and enables its consistent application across North America, Western and Central Europe (**Paper 6**). Based on my research, the return to the application of Upper *duplicata* (or equivalent *Siphonodella (Si.) mehli* Zone, Becker et al. 2021 or *Si. cooperi*, Hogancamp et al. 2019) is challenging for the rare occurrence of the index species *Siphonodella (Si.) mehli* (=*Si. cooperi* M1) outside of North America, and this species is descendant of *Siphonodella wilberti* (**Paper 6**). Further argument for application of the *Siphonodella wilberti* Zone is that the FO of "east European" *Si. belkai* coincides with the FO of *Siphonodella wilberti* in both the Rhenish Massif and Moravian Karst (**Paper 5**). This enables correlation of the regional *Siphonodella belkai* Zone with the base of the *Siphonodella wilberti* Zone of the cosmopolitan group (Fig. 5). This allows more precise correlation of lower Tournaisian biozones between North America, Western, Southern and Central Europe, and the East European and Uralian regions.

2.2.2 Refinement of the lower Tournaisian Carbon Isotope Stratigraphy

Combined with conodont biostratigraphy, carbon isotope ($\delta^{13}C$) stratigraphy provides an important independent method for stratigraphic correlation in the Carboniferous (e.g. Saltzman and Thomas 2012). The lower Carboniferous $\delta^{13}C$ record shows two major positive excursions in the Tournaisian: the Hangenberg Crisis excursion and the mid-Tournaisian Isotopic Excursion (TICE; Yao et al. 2015). Both excursions are well established as interregional correlation tools (Saltzman et al. 2000; Saltzman 2002; Saltzman and Thomas 2012; Kaiser et al. 2006, 2008, 2015; Kumpan et al. 2014ab, Rakociński et al. 2021, 2023). Several weaker positive $\delta^{13}C$ excursions had been

reported from the lower Tournaisian interval between these two events (Buggish et al. 2008; Qie et al. 2011, 2016; Kumpan et al. 2014b; Plotitsyn et al. 2024), but their interregional significance had not been systematically tested and supported. My research provided support for the interregional correlative significance of the lower Tournaisan small-scale excursions in the study of lower Tournaisian limestones in the Moravian Karst in Moravosilesian Basin, Czechia (Fig. 1; **Paper 7**).

Stable carbon isotope composition was analysed using Thermo Scientific DELTA V mass spectrometer (J. Frýda; Czech Geological Survey, Prague) in the Lesní lom, Mokrá and Křtiny sections north-east to Brno, Czechia. All the values are reported in ‰ relative to V-PDB by assigning a $\delta^{13}C$ value of +1.95 ‰ and a $\delta^{18}O$ value of 2.20 ‰ to IAEA-NBS-19. Diagenetic screening using Mn/Sr, Y/Ho and correlations between $\delta^{13}C$, $\delta^{18}O$, Mn/Sr and TOC indicates that the primary marine $\delta^{13}C$ signal is largely preserved in the Lesní lom and Mokrá sections, enabling reliable chemostratigraphic interpretation; the absolute values in the Křtiny section are probably lowered by diagenesis, but the overall stratigraphic pattern is preserved (for methodological detail see **Paper 7**).

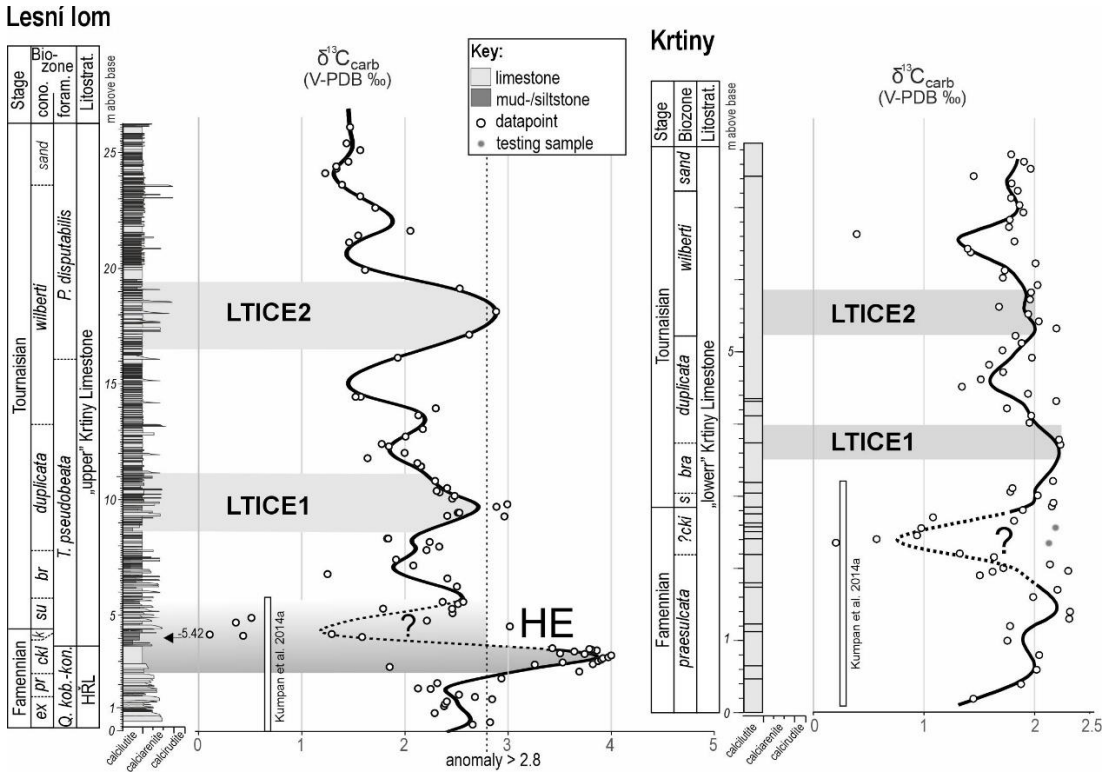

Figure 7. Stratigraphic columns of the studied Lesní lom and Křtiny sections showing chronostratigraphy, conodont and foraminiferal biostratigraphy, lithostratigraphy, lithology, and $\delta^{13}C$ data with predictive smoothing spline. Abbreviations - carbon isotopic excursions: HE – Hangenberg carbon isotopic excursion; LTICE – Lower Tournaisian carbon isotopic excursions. HŘL – Hády-Říčka Limestone.

Three small-scale excursions have been identified above the prominent Hangenberg Event Isotopic Excursion, designated LTICEs (Lower Tournaisian Isotopic Carbon Excursions): LTICE1 in the *Siphonodella duplicata* Zone, LTICE2 in the *Siphonodella wilberti* Zone, and LTICE3 at the *Si. sandbergi/Si. quadruplicata* conodont zones boundary (Figs. 7 and 8). LTICE1 and LTICE2 are correlated between two facies successions of the Moravian Karst Unit, the calciturbiditic Horákov and hemipelagic Hostěnice facies (Fig. 7). This correlation confirms stratigraphic robustness independent of facies (**Paper 7**).

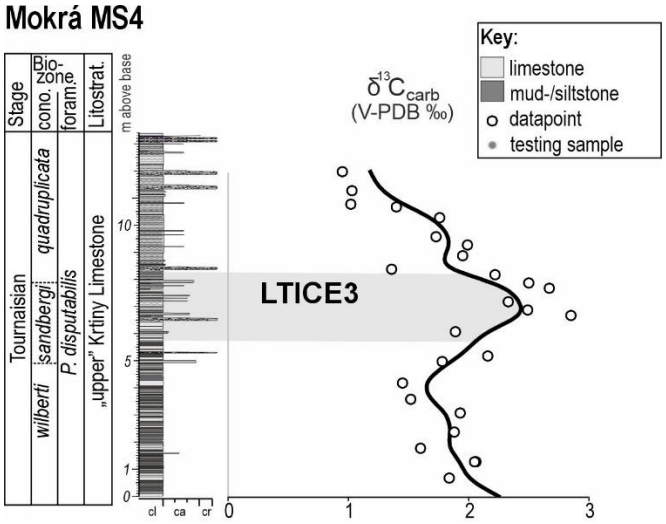

Figure 8. Stratigraphic columns of the studied Mokrá section showing chronostratigraphy, conodont and foraminiferal biostratigraphy, lithostratigraphy, lithology, and $\delta^{13}C$ data with predictive smoothing spline. For abbreviations see Fig. 7.

Interregional correlation of the three LTICEs establishes their potential as correlative markers complementary to conodont biozonation, well documented for Paleotethys Realm (Fig. 9). LTICE1, LTICE2 and LTICE3 correlate with positive excursions in the North Urals (Plotitsyn et al. 2024), South China (Qie et al. 2015, 2016). LTICE1 and LTICE2 are correlated with excursions in the Namur-Dinant Basin, Belgium (**Kumpan et al. 2014b**), whereas LTICE3 is probably not preserved due to the diagenetic reasons. LTICE2 and LTICE3 are tentatively correlated with Kinderhookian excursions from the Burlington Shelf, Iowa, in Panthalassan Realm (Stolfus et al. 2020).

The positive $\delta^{13}C$ excursions LTICEs 1–3 occur in lowstand deposits in the Moravian Karst (**Paper 7**), evidenced by higher abundance of calciturbidites derived from inner-mid ramp zones. The similar situation was also documented in the Namur-Dinant Basin, where are these excursions tied with regressive deposits (**Kumpan et al. 2014b**). An enhanced continental weathering during lowstands likely increased nutrient delivery to the oceans, stimulating productivity and organic carbon burial. This is consistent with interpretations of the mid-Tournaisian Isotopic Carbon Excursion

(TICE; Yao et al. 2015; Qie et al. 2023). I interpreted these sea-level falls as climatically driven, suggesting that at least three small-scale glaciation events occurred during the early Tournaisian, between the Hangenberg and mid-Tournaisian glaciation events (Fig. 10; **Paper 7**). This interpretation, however, should be tested by high-resolution $\delta^{18}O$ phosphate paleothermometry.

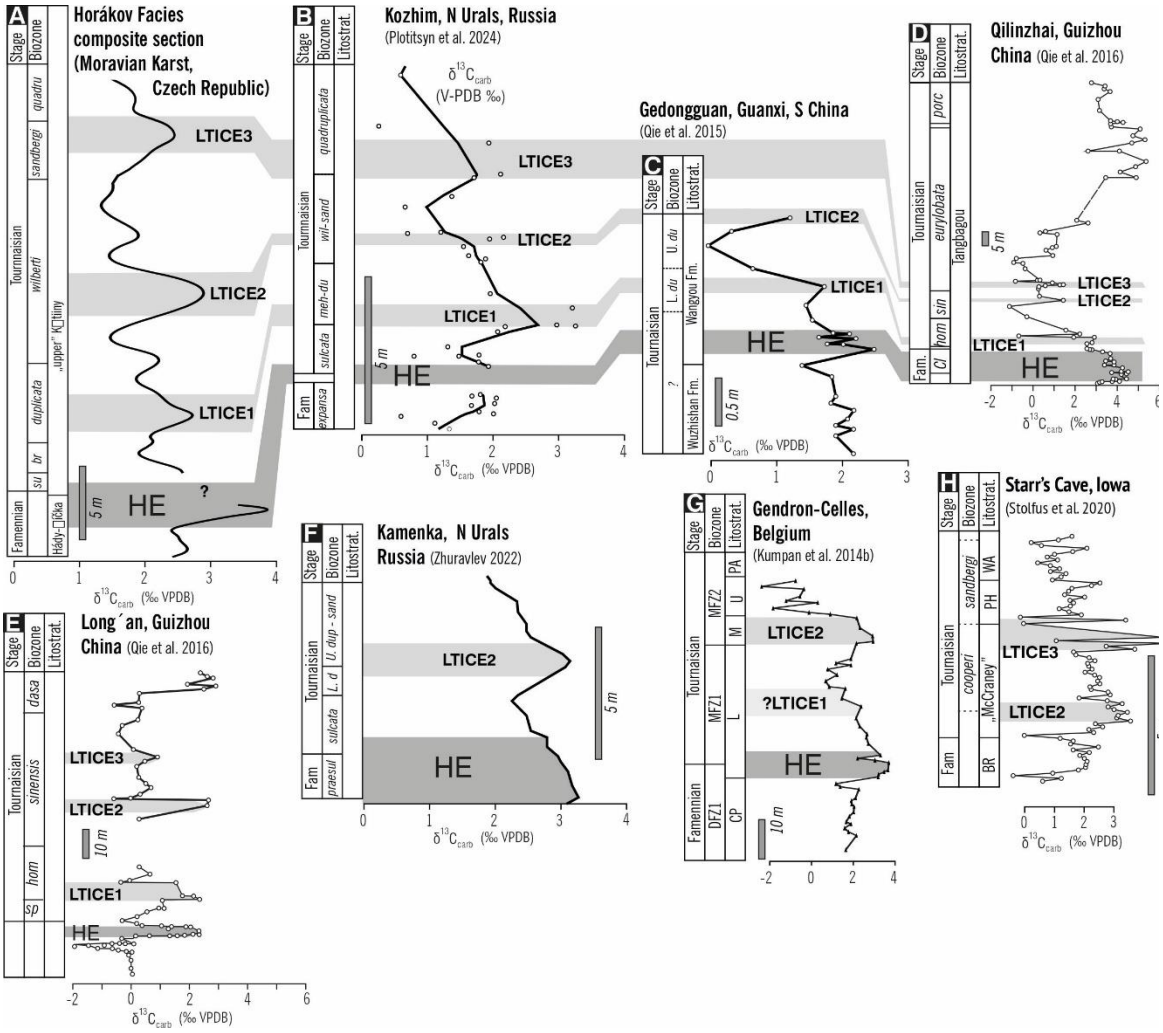

Figure 9. Chemostratigraphic correlation of the lower Tournaisian Moravian Karst Composite δ13C curve with curves from other sections of the Palaeotethys Realm-related deposits (Urals, South China, Namur-Dinant Basin) as well as Panthalassan Realm (Burlington Shelf). The *Siphonodella cooperi* Zone (Iowa, Fig. 9H; Stolfus et al. 2020) corresponds to the Upper *duplicita* Zone (*sensu* Sandberg et al. 1978).

Unlike the major Hangenberg and mid-Tournaisian events, these small-scale carbon cycle perturbations do not appear to have caused significant ecosystem

turnovers; they coincided instead with a period of conodont diversification in the *Siphonodella wilberti* and *Si. sandbergi* zones (Fig. 10), suggesting that early Tournaisian recovery fauna had developed greater ecological resilience in the aftermath of the Hangenberg Crisis (**Paper 7**).

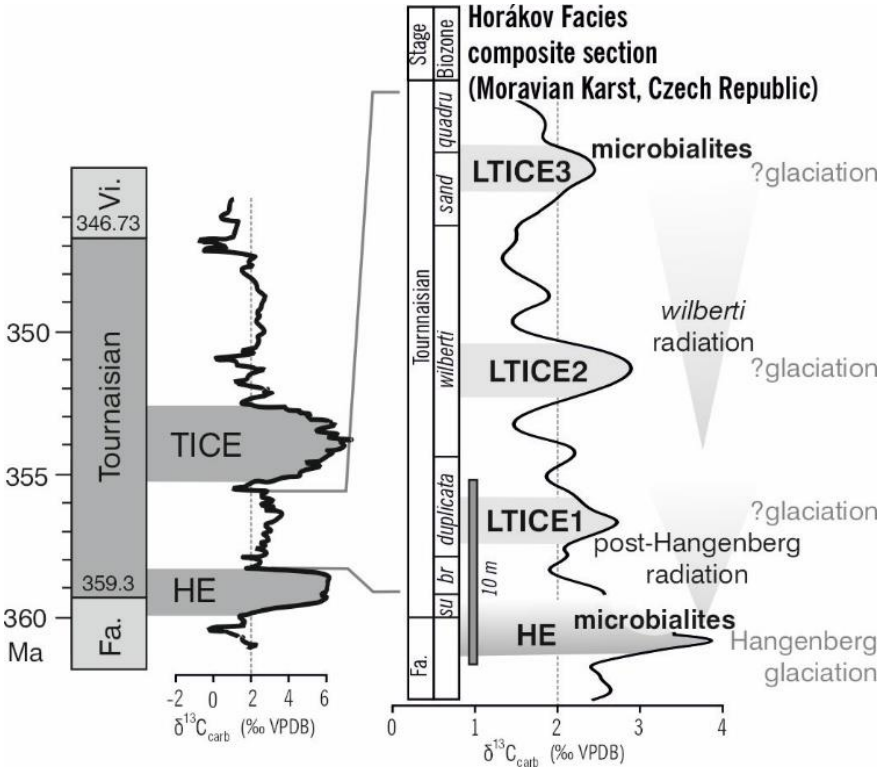

Figure 10. Composite section showing the Lower Tournaisian $\delta^{13}C$ excursions (LTICE) in the context of major isotopic fluctuations (Cramer & Jarvis 2020), inferred glaciation events, conodont evolutionary events, and the occurrence of disaster facies (microbial-rich facies in the Moravian Karst). Abbreviations: su – *sulcata*; br – *bransoni*; sand – *sandbergi*; quadru – *quadruplicata*; Fa. – Famennian; Vi. – Viséan.

2.2.3 Conclusive remarks

By combining conodont biostratigraphy with carbon isotope chemostratigraphy in the Moravian Karst sections, my research has produced an integrated stratigraphic framework for the lower Tournaisian with broader interregional correlation potential (Fig. 9). The taxonomic revision of siphonodellides resolved nomenclatural issues and enabled consistent application of the biozonation across North America, Western and Central Europe, and the East European-Uralian regions (Fig. 5), including the first documentation of the eastern European siphonodellid group outside its typical areas, and two new species *(Siphonodella kalvodai, Siphonodella* sp. A). The chemostratigraphic study identified three small-scale $\delta^{13}C$ excursions (LTICEs) between the Hangenberg and TICE events, established their interregional significance, and linked them to glacioeustatic lowstands (Fig. 10).

3 Element geochemistry in Paleoenvironmental reconstruction: from black to red deposits

While the preceding chapter employed geochemical proxies primarily as stratigraphic correlation tools, the focus of the second thesis part shifts towards their application for paleoenvironmental interpretation. This part summarizes my main contributions to research of Paleozoic carbonate producing environments, which is based on a series of **papers 8-15** employing multiproxy geochemical approach to reconstruct sea-water chemistry, particularly redox conditions, continental weathering and runoff, bioproductivity changes, as well as magmatic hydrothermal activity and hydrographic basin regime.

These studies are presented in two topics, distinguished by two contrasting sedimentary products of marine redox spectrum: **organic-rich black carbonates**, where reducing conditions typically concentrate redox-sensitive metals and organic matter, and **iron-rich red carbonates**, organic-matter poor deposits, where complex redox conditions fixed iron as oxides. As depositional expressions of redox-driven processes, both sediment types carry geochemical signatures reflecting a combination of primary marine environmental conditions and subsequent diagenetic overprint. My aim was to separate these two signals and contribute to understanding the causes and nature of processes and events responsible for producing these remarkable deposits.

Element geochemistry is widely used to reconstruct paleoenvironmental and climatic conditions prevailing during and after deposition. No single proxy alone provides robust evidence for any paleoenvironmental feature and only a combination of proxy types allows reliable reconstruction (Craigie 2018; Algeo and Li 2020). The application of detrital proxies as a chemostratigraphic tool was presented in section 2.1. Among the most widely applied detrital proxies are Al, Ti, Th, and Zr, being resistant to mobilization during diagenesis and weathering, reflecting their predominantly lithogenic origin (McLennan 2001). However, aution is required where these elements are hosted in volcanogenic (Racki et al. 2019) or microbially mediated autigenic fraction (**Vodrážková et al. 2025**). Redox-sensitive trace elements (RSTE) - including Co, Cu, Mo, Ni, Pb, U, V and Zn - become enriched in sediments under reducing conditions (Tribovillard et al. 2006; Algeo and Li 2020; Algeo and Liu 2020; Smrzka et al. 2019). Their enrichment patterns depend on the host sediment fraction: Mo, V and Zn are preferentially associated with organic matter, while Co, Cu, Ni and Pb show stronger association with the sulfide fraction (Algeo and Liu 2019). Enrichment factors (EFs), calculated by Al-normalisation relative to average upper continental crust or average shale, quantify authigenic enrichment under reducing conditions (Tribovillard et al. 2005). Complementary to RSTE, rare earth elements (REE) provide an independent proxy set particularly valuable for carbonates, where RSTE enrichments may be obscured by dilution

or diagenesis. The distribution of REEs in marine sedimentary rocks can provide insights into ancient seawater geochemistry (Elderfield et al. 1990; Bau and Dulski 1996; Smrzka et al. 2019) and ocean redox conditions (Tostevin et al. 2016), though their application assumes that carbonate-bound REE are resistant to diagenetic alteration. Particularly, cerium and europium anomalies are widely used. However, their application requires careful evaluation in ancient carbonates (Zwicker et al. 2018; Zhang and Shields 2022, 2023).

A recurring methodological challenge in paleoenvironmental reconstruction is the resolution of the analytical method applied. Bulk-rock geochemistry averages signal across various carbonate and non-carbonate rock components and can mask or obliterate geochemical contrasts that develop at the scale of individual carbonate phases bearing different paleoenvironmental signal, e.g. micrites, cements, bioclasts, microbialites. *In situ* LA-ICP-MS targeted at individual grains resolves this problem by providing element distributions at the scale of microfabrics. On the other hand, bulk geochemistry provides a practical means of tracking stratigraphic trends over longer time intervals, where LA-ICP-MS analysis would be prohibitively demanding. The two approaches are thus complementary and developed across my studies commented in following topics.

3.1 Topic C: Hangenberg Crisis and its anoxic black deposits

As stressed in the section 2.1, the Hangenberg Crisis (Fig. 2) was series of global events that led to mass exctinction, representing the natural DCB (Walliser 1985). The Hangenberg Crisis was associated with the first massive Devonian Gondwana glaciation, evidenced by oxygen isotope paleothermometry, glacial deposits dated by palynomorphs, and widespread regressive marine sediments and stratigraphic gaps (Isaacson et al. 2008; Lakin et al. 2016). A clear connection exists between the biocrisis, climatic shift, and extensive global marine anoxia. However, the triggers and mechanisms of anoxia development remain still incompletely understood.

The origin of anoxic black shale deposits during the crisis has been interpreted in contrasting ways. Some studies proposed that anoxic bottom waters were pushed onto shelves by transgression e.g. Caplan and Bustin 1999; Becker et al. 2016; Kaiser et al. 2015), supported by onlap geometry of the Hangenberg Black Shale on pre-crisis units (Becker et al. 2021). In the **paper 3**, we argued for regressive anoxic deposits driven by enhanced paleoproductivity from increased continental runoff related to glacioeustatic fall, also evidenced by Carmichael et al. (2016). The regressive interpretation was supported by higher sedimentation rates in Hangenberg Crisis deposits and non-uniform timing of onset of anoxic conditions across European sections (**Paper 3**). The diachronous onset of late Famennian anoxia was also highlighted by Hedhli et al. (2023), who suggested that the Hangenberg Black Shale Event did not represent a true

oceanic anoxic event, but rather reflected widespread anoxia developed in numerous tectonically isolated Black Sea-type basins formed during advancing orogeneses, further supporting a regressive model.

The source of elevated nutrient fluxes for organic-rich shale deposition is a separate question. Terrestrial forestation and intensification of continental weathering represent an increasingly supported long-term trigger for increased sourcing (Algeo and Scheckler 1998; Qie et al. 2023;), operating on timescales of millions of years. Volcanic nutrient input of nutrients has been also proposed, questioned series of local sources *vs* large igneous province (**Papers 8** to **10**; Rakociński et al. 2020, 2021). Additionally, the possibility of supernova-triggered ozone depletion, inferred from malformed plant spores, has been raised (Marshall et al. 2020; Fields et al. 2020), but remains highly speculative.

In the following section I synthesize three case studies addressing this problem at progressively increasing spatial scales: from microscale geochemical signals in a single carbonate section of the Moravian Karst, Moravosilian Basin Czechia (**paper 8**) through regional comparison of two European basins (Moravosilesian and Namur-Dinant basins; **paper 9**), to intercontinental correlation (Europe and China) of mercury anomalies (**paper 10**). Together, they document paleoredox conditions and their temporal evolution, basin paleohydrography and connectivity, records of magmatic and volcanic activity, and productivity changes during this critical interval.

3.1.1 Geochemical record of Hangenberg anoxia in the Moravian Karst

In the Moravian Karst, the Hangenberg Black Shale Event is preserved in an unusual facies. Rather than the organic-rich black shales typical of the event in shelf and epicontinental settings, the lower slope environment recorded a dark-grey to black laminated limestone - "laminite" - whose origin and paleoenvironmental significance long remained debated (Fig. 11). This facies provided a rare opportunity to investigate the geochemical fingerprint of the Hangenberg Black Shale Event in a carbonate archive largely free of detrital dilution, in great thickness around 1 m (most of the limestone equivalents of the Hangenberg Black Shale Event are strongly condensed; e.g., **Paper 1**), and to assess whether anoxic conditions characteristic of the event were expressed even in settings where black shale deposition did not occur (**Paper 8**).

The laminite unit at the top of the Famennian Hády-Říčka Limestone of the Líšeň Formation was documented at Lesní lom, Mokrá and Říčka Brook Valley (Kalvoda et al. 1987; Kumpan et al. 2014a; **Paper 2**). In this study (**Paper 8**), I combined carbonate petrography, scanning electron microscopy and *in situ* LA-ICP-MS on the laminite and the underlying pre-event calciturbidite from the Mokrá-eastern quarry, where is located the best outcrop. Twenty line scans parallel to lamination were measured on two polished limestone slabs (Fig. 11) using an Analyte G2 excimer laser ablation system coupled to an Element 2 sector-field ICP-MS (Department of Chemistry, Masaryk

University), with a 150 μm spot size. This analytical setup allowed to document element distributions t at the scale of individual laminae and microfabric domains rather than averaged across the bulk sample.

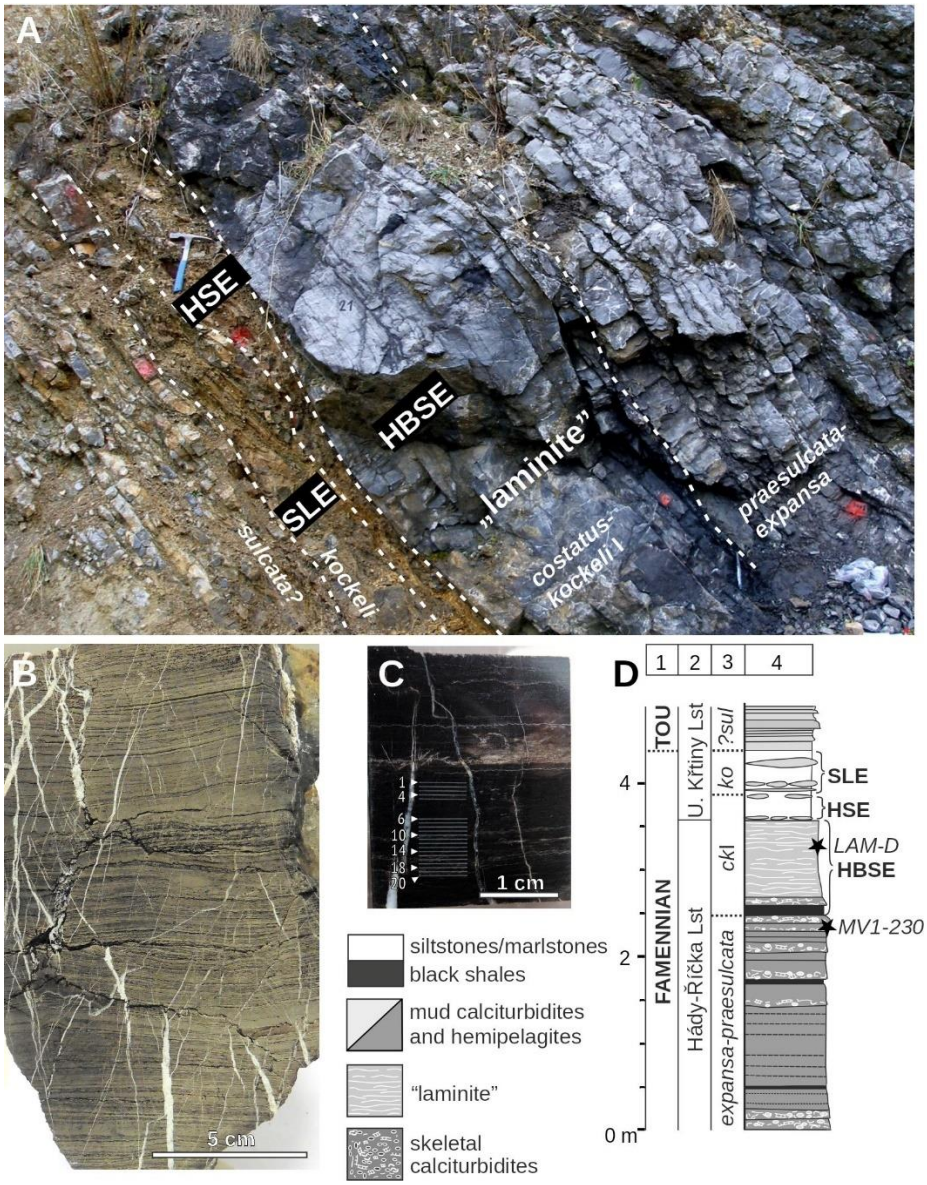

Figure 11. (A) Field photograph of the studied overturned Devonian–Carboniferous interval at the Mokrá-east quarry (section MV1); (B) etched surface of a laminite sample; (C) polished laminite sample showing measured lines; (D) stratigraphic log of the studied section (1 – chronostratigraphy; 2 – conodont biozones; 3 – lithostratigraphy; 4 – lithological log). Abbreviations: TOU – Tournaisian; ckI – *costatus-kockeli* Interregnum; ko – *kockeli* Zone; ?sul – ?*sulcata* Zone; HBSE – Hangenberg Black Shale Event; HSE – Hangenberg Sandstone Event; SLE – Stockum Limestone Event.

The laminite facies comprises three distinct microfacies: bindstones (MF2), peloidal grainstones (MF3) and bioclastic packstones to lime mudstones (MF4), with MF3 and MF4 occurring as thin turbiditic intercalations within the dominant bindstone MF2. MF2 displays features indicative of microbial origin: irregular laminae of dense micrite and microsparite, flaser-like fabric, asymmetric automicritic peloids with clotted peloidal texture and coccoidal fabrics, and dissolution seams of insoluble residues.

REE compositions of the laminite and pre-event calciturbidite show only limited early diagenetic overprint and fall within or close to the seawater field in discriminating biplots (**Study 10**). The calciturbidite displays a prominent UCC-normalised MREE bulge, consistent with Fe-Mn oxyhydroxide redox cycling via a particulate shuttle, while the overlying laminite shows LREE depletion and progressive HREE enrichment (Fig. 12a) similar to modern seawater and Devonian microbialites from the Canning Basin, Australia (Nothdurft et al. 2004), reflecting dominance of authigenic carbonate phases.

Positive Eu anomalies (Bau 1991), and very low Al/(Al+Fe+Mn) ratios (Boström 1983; Racki et al. 2002) in both units suggest influence of reduced high-temperature hydrothermal fluids, possibly related to latest Devonian rift magmatism in the eastern Rhenohercynian Zone (Přichystal 1993; Janoušek et al., 2014).

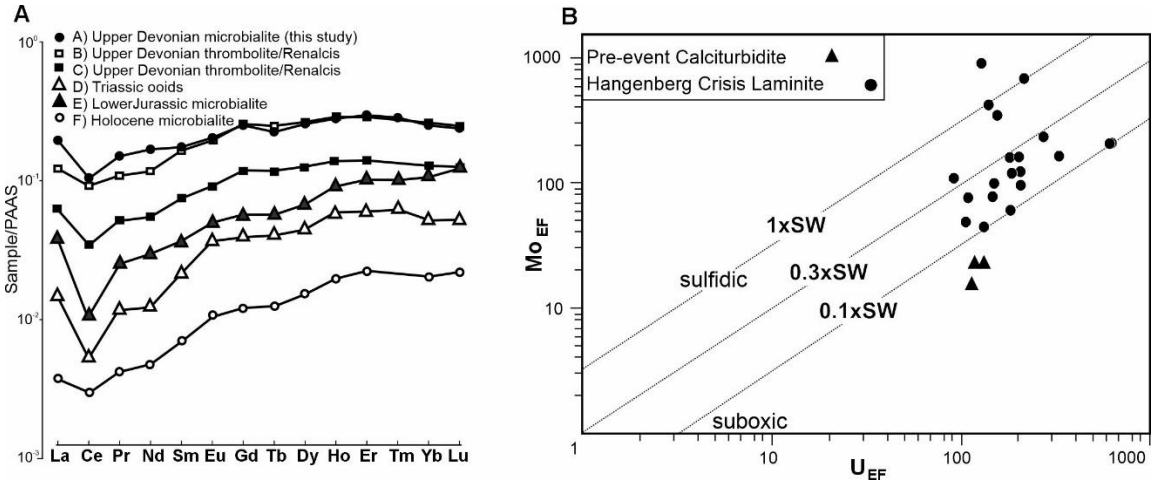

Figure 12. (A) Crossplot of MoEF vs. UEF of analyzed calciturbidite and laminite samples (modified from Algeo and Tribovillard, 2009). (Mo/U)SW = 3.1. (B) Mean REE concentrations normalized to PAAS for the latest Devonian laminite (MV1-LAMD), Late Devonian microbialites (highest values and mean of 16 samples; Leonard Shelf, Australia; Nothdurft et al., 2004), Early Triassic ooids (Li et al., 2017), Early Jurassic microbialites (average of 15 samples; Della Porta et al., 2015), and Holocene microbialites (average of 52 samples; Great Barrier Reef; Webb and Kamber, 2000).

Mo and U enrichment factors show elevated values and covariation patterns reflecting high-frequency episodic shifts between oxic, suboxic and ferruginous anoxic

bottom conditions (Fig. 12b; Algeo et al. 2007; Algeo and Tribovillard 2009) during laminite deposition. These rapid redox fluctuations likely represented a major environmental stress factor during the Hangenberg Crisis, repeatedly exposing benthic communities to alternating redox conditions. Comparable redox instability has been documented from the Hangenberg interval in southern Poland, where Marynowski et al. (2012) interpreted intermittent oxygenation superimposed on predominantly anoxic conditions, suggesting that fluctuating oxygen deficiency was an important regional to possibly global control on latest Devonian marine ecosystems.

Such instability may have suppressed normal skeletal carbonate production and promoted proliferation of microbial and authigenic facies characteristic of post-extinction "anachronistic" environments. The Hangenberg microbial-authigenic laminite together with overlying lower Tournaisian ooidal and micritic limestones represents a typical anachronistic facies sequence comparable to globally documented post-extinction carbonate successions, including those following the end-Permian mass extinction (e.g., Woods 2014).

3.1.2 Paleoredox evolution at regional scale: basin restriction and magmatic forcing

The high-frequency redox oscillations and indirect evidence for hydrothermal input documented in the lower interval of the Hangenberg Crisis deposits in the Moravian Karst raised questions about whether similar patterns of paleoredox evolution and magmatic forcing were expressed at larger scale and in other basins. To investigate this, a multi-proxy geochemical study (**Paper 9**) was conducted across three DCB sections of Laurussia related basins: Lesní lom in the Moravian Karst, Czechia (slope settings), and Gendron-Celles and Les Ardennes sections in the Ardennes, Namur-Dinant Basin, Belgium and France (neritic homoclinal ramp settings) (Fig. 1). I have analysed and interpreted bulk major and trace element geochemistry dataset analyzed by ICP-MS/OES (Bureau Veritas, Vancouver).

Correlatable patterns of detrital proxies are recognisable between both basins, with abrupt increases in Zr/Al and Ti/Al marking the base of the middle Hangenberg Crisis interval (Hangenberg Sandstone Event) (Fig. 13), consistent with the chemostratigraphic framework developed in **Paper 3**. Several levels display anomalously high absolute values of Zr/Al_2O_3 together with elevated TiO_2/Al_2O_3 and Fe/Ti above average crustal values (McLennan 2001) and low Al/(Al+Fe+Mn) (Fig. 13; **Paper 9**). These elemental ratio proxies were used in several publications as indication of volcanic and hydrothermal source (Boström 1983; Racki et al. 2002, 2019; Racki 2020; Pujol et al. 2006). The data imply derivation of part of the detrital fraction from coeval magmatic rocks in the Rhenohercynian domain (Přichystal 1993; Janoušek et al. 2014; Raumer et al. 2017), with a possible additional hydrothermal contribution.

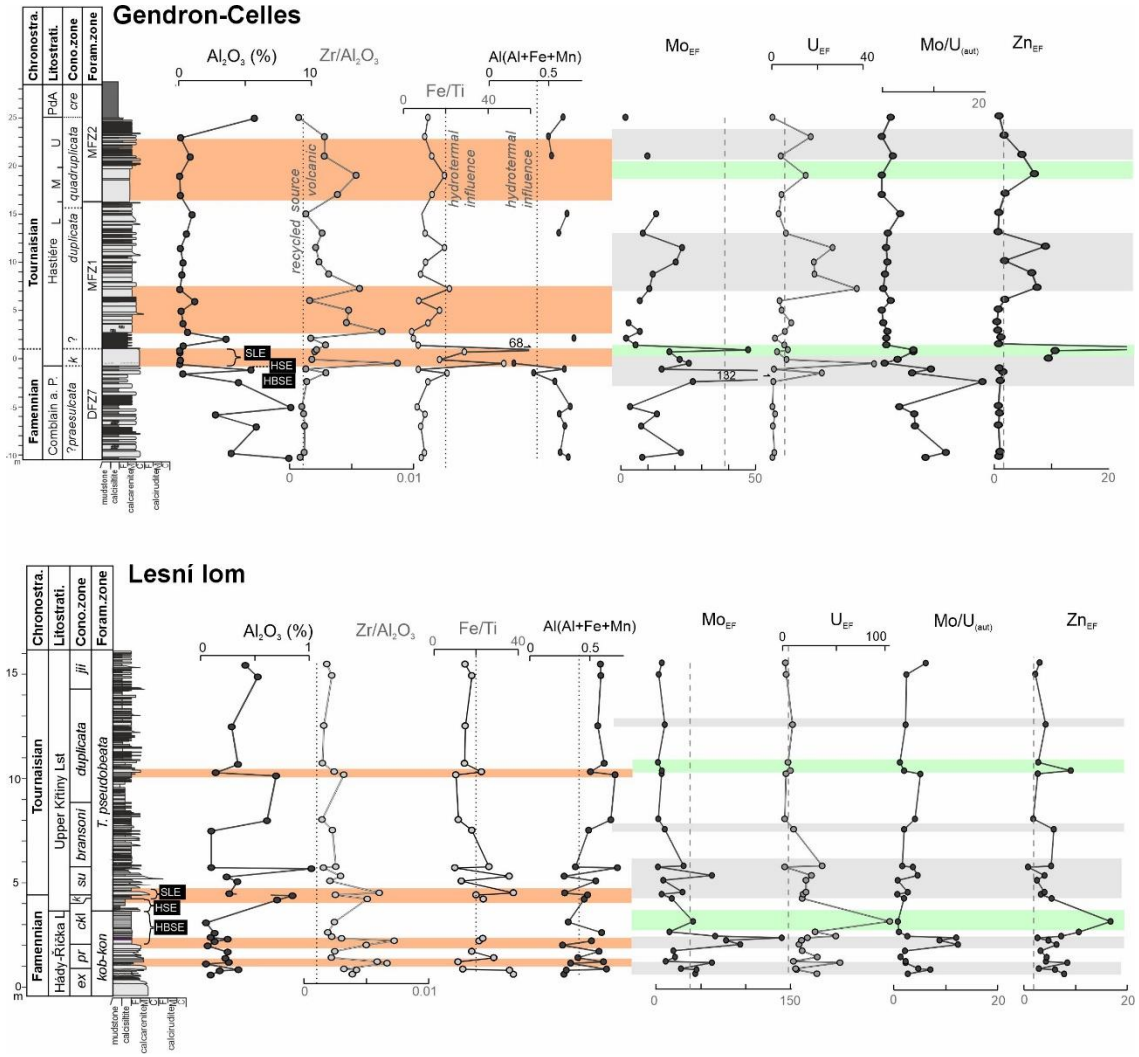

Figure 13. Vertical distribution of selected geochemical proxies from limestones at the Gendron-Celles (Belgium) and Lesní lom (Czechia). Detrital, volcanic, and hydrothermal input proxies; pale brown boxes - levels indicating coarsening of the detrital phase and/or volcanic/hydrothermal input. Paleoredox and paleoproductivity proxies; grey boxes - decreased oxygenation with increased paleoproductivity; green boxes - increased paleoproductivity. Abbreviations: HBSE – Hangeberg Black Shale Event, HSE – Hangenberg Sandstone Event, SLE – Stockum Limestone Event (conodont zones abbreviations see Fig. 4).

The covariation of enrichment factors of Mo and U (Algeo and Tribovillard 2009) reveal systematic changes in redox conditions across the uppermost Famennian and lower Tournaisian in both basins (Fig. 14). In the Moravian Karst (Fig. 14a), the pre-crisis Famennian MoEF and UEF indicate an unrestricted marine trend converging with that of restricted systems, with redox conditions ranging from suboxic to euxinic. The top of the Famennian records alternating suboxic to anoxic conditions compatible with the transgression of the Hangenberg Black Shale Event. In the Tournaisian, MoEF and UEF oscillate between oxic and anoxic conditions along a vector of strongly

restricted marine conditions, supported by Mo/TOC proxy data. In the Namur-Dinant Basin (Figs. 14bc), three stratigraphically distinct levels of elevated MoEF and UEF were identified, with covariation vectors indicating: 1) weakly restricted pre-crisis conditions with Fe-Mn redox cycling; 2) unrestricted to weakly restricted uppermost Famennian conditions with alternating suboxic to anoxic redox; 3) and strongly restricted lower Tournaisian conditions with prevailing suboxic redox (**Paper 9**). Comparable paleohydrographic patterns were documented from the Appalachian Basin (Algeo et al. 2007).

Basin restriction, reflected in the Mo/U systematics, intensified progressively through the crisis and dominated the lower Tournaisian geochemical record (Fig. 14d), driven by glacioeustatic sea-level fall (Isaacson et al. 2008) and advancing Variscan and Acadian tectonics. The early Tournaisian basin restriction in the Moravo-Silesian Na-

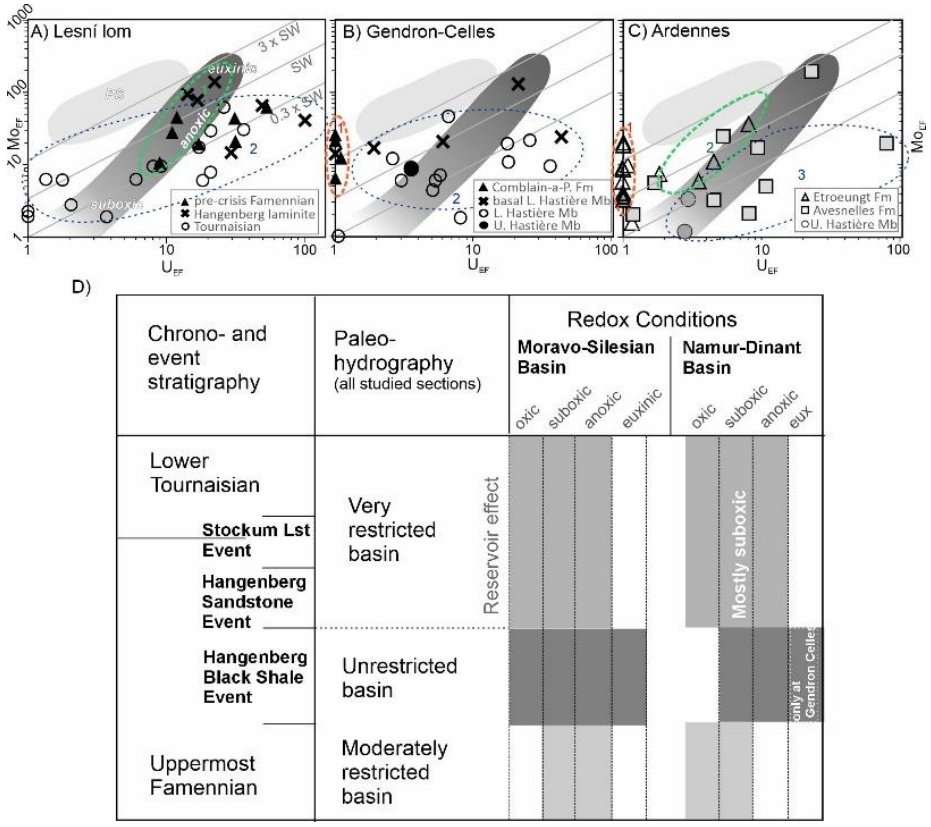

Figure 14. Paleohydrographic and redox changes across the Devonian–Carboniferous boundary interval in the Moravian Karst (Moravo-Silesian Basin, MSB) and Namur-Dinant Basin (NDB). Abbreviations: HBSE – Hangenberg Black Shale Event; HSE – Hangenberg Sandstone Event; SLE – Stockum Limestone Event; PS – particulate shuttle.

mur-Dinant, and Appalachian Basin suggest that glacioeustatic fall produced a broadly correlatable restriction signal across geographically distant basins. However, the

variable onset and intensity of anoxia between sections indicates that local tectono-magmatic processes and basin geometry significantly modulated the regional expression of this signal, as stressed by Hedhli et al. (2023).

The main finding of the study is the coincidence of elevated volcanic, hydrothermal and detrital input proxies with peaks in paleoproductivity indicators (Fig. 13), suggesting that continental runoff and magmatic activity contributed to nutrient supply, driving enhanced organic productivity and oxygen drawdown during the Hangenberg Crisis. Combination of glacio-eustatic and tectonic basin restriction in the early Tournaisian then reduced deep-water renewal and limited the resupply of oxygen and trace elements, as documented from the Moravo-Silesian, Namur-Dinant and Appalachian basins. The MoEF and UEF covariation patterns indicating basin restriction above the Hangenberg Zr/Al peak (Figs. 13 and 14) may therefore serve as orientation criteria for DCB redefinition.

3.1.3 Mercury anomalies as tracers of magmatic activity

The geochemical evidence for magmatic activity at around DCB identified at both the microscale (Moravian Karst laminite) and regional scale (bulk geochemistry of two Laurussia marginal basins) relied on proxies reflecting volcanic and hydrothermal input to the sediment but not uniquely fingerprinting volcanic degassing at a larger scale. Mercury chemostratigraphy offers a more direct test: Hg enrichments in sedimentary records are used to trace volcanic activity during the mass extinction events (e.g., Sanei et al., 2012; Sial et al. 2013; Percival et al. 2015; Racki et al. 2019), because Hg is volatilised during volcanic degassing and deposited globally via atmospheric transport.

The **paper 10** presents my investigation of Hg chemostratigraphy and other trace element contents across the DCB with the aim of detecting Hg enrichments and possible large-scale magmatic activity during the Hangenberg Crisis. It represented the first detailed Hg chemostratigraphic study of the DCB, coeval with Paschall et al. (2019). It followed the methodological work of Racki et al. (2018), which was focused primarily on the Frasnian–Famennian boundary, while also including preliminary DCB data. Two geographically distant sections were studied in **paper 10**: Lesní lom in the Moravian Karst, Moravosilesian Basin, Czech Republic, and Duli in Guangxi Platform, South China (Fig. 1). Bulk-rock geochemistry was determined by ICP-MS/OES (Bureau Veritas, Vancouver); mercury concentrations were subsequently refined by atomic absorption spectrometry (AMA254 analyzer, Czech Geological Survey, Prague; detection limit >5 ppb, repeatability ~5%), and TOC was quantified by flash combustion elemental analysis after HCl decarbonation (Czech Geological Survey, Prague).

The studied sections differ markedly in their Hg sequestration pathways. At Lesní lom, Hg correlates with excess iron and TOC, indicating sequestration primarily via pyrite and organic matter under oscillating redox conditions. The low TOC values

(generally < 0.1 wt%) render Hg/TOC ratios unreliable as a volcanic proxy, and Hg/Fe_{xs} is therefore preferred as the normalisation ratio. The excessive Hg (high Hg/Fe_{xs}) was documented before and with the lower crisis interval (Fig. 15). At Duli, by contrast, Hg correlates strongly with Al and Fe but not with TOC or sulphur, indicating transport by clay-bound terrigenous detritus of volcanic origin; the Hg enrichment was also identified below and within the lower crisis interval (Fig. 15). High Hg enrichment to 89 (Fig. 15) points to a significantly elevated volcanic Hg flux, consistent with high abundance of zircons in the shale. Comparable anomaly was reported from South China Block, NE Vietnam (Paschall et al. 2019) and Kazakhstan (Rakociński et al. 2021), and direct volcanic evidence was provided by study of tuffs within the Hangenberg Crisis interval (concordia age of 359.6 ± 1.9 Ma; *kockeli* conodont Zone; Liu et al., 2012) at Dapoushang section, Guizhou province.

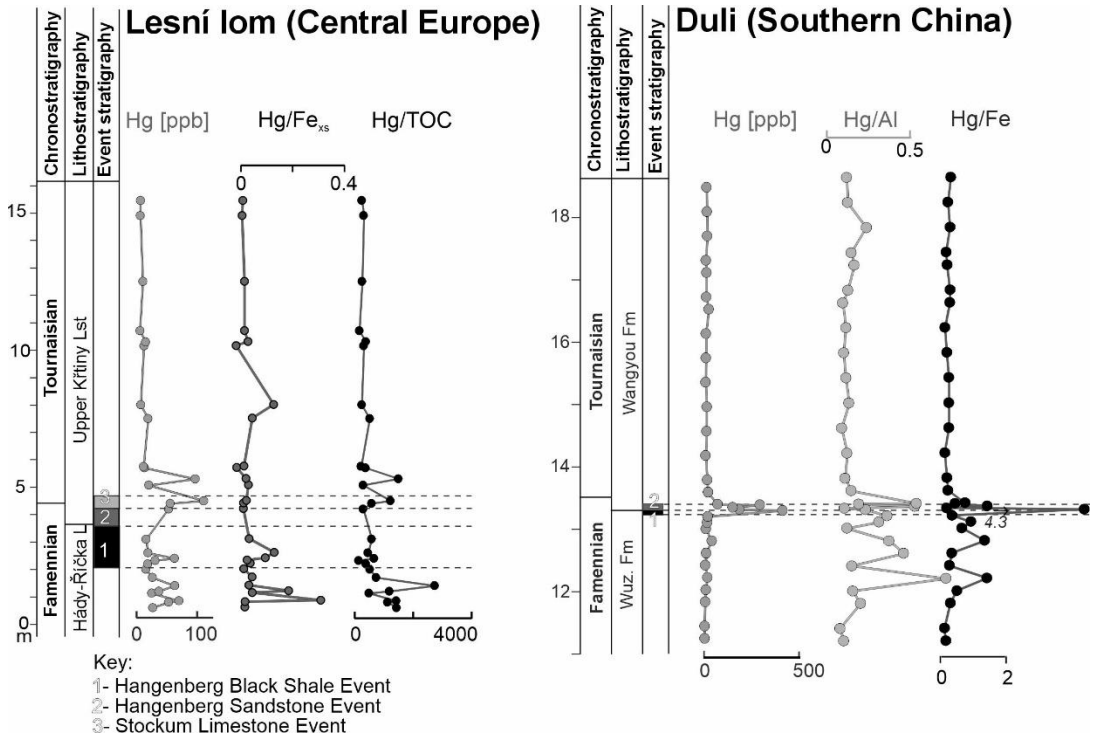

Figure 15. Vertical distribution of selected mercury ratios in the studied sections at Lesní lom (Czech Republic) and Duli (South China).

The widespread nature of these geochemical anomalies and lithological evidence across geographically distant areas suggests involvement of a more extensive volcanic source beyond local Rhenohercynian extensional magmatism. The multi-phase Viluy Large Igneous Province on the Siberian Platform has a phase (364.4 ± 1.7 Ma) that slightly precedes the observed Hg anomalies and the Hangenberg Crisis (Ricci et al.

2013). The available evidence therefore favours a multi-source model in which regional Rhenohercynian extensional magmatism provided a persistent background hydrothermal Hg flux to the Moravo-Silesian Basin, while a more distal (large igneous province related?) source contributed the elevated Hg anomaly recorded simultaneously in the South China Block.

3.1.4 Conclusive commentary

My multidisciplinary research demonstrates that the development of marine anoxia during the Hangenberg Crisis cannot be explained by a single mechanism. The micro- to regional-scale geochemical record supports a combined model in which continental runoff and magmatic nutrient input, basin restriction, and volcanic degassing acted together, but with different timing and relative importance across basins. The magmatic signal identified at the microscale in the Moravian Karst laminite finds its regional counterpart in detrital proxy ratios showing volcanic source across two European basins, and its global expression in mercury anomalies recorded in central Europe and South China. The results demonstrate that Hg anomalies and other geochemical proxies must be interpreted in the context of host-phase control and basin-specific processes, rather than as simple global signals.

3.2 Topic D: Geochemistry of Paleozoic Red Iron-rich Marine Sediments

In this section, I extend the geochemical approach from anoxic systems to oxidizing environments, focusing on the deposition and diagenesis of red marine carbonates. The preceding **papers 8 to 10** on the Hangenberg Crisis were focused on geochemical signals preserved in anoxic black deposits, where reducing conditions concentrated redox-sensitive metals in sulphides or organic matter. Marine red beds represent different case: sediments deposited under complex oxidizing-reductive conditions where iron and other elements are fixed as oxides rather than mobilised into solution or sulphides. The following **papers 11 to 15** examine four Ordovician and Devonian marine red bed successions using *in situ* LA-ICP-MS to resolve precipitation processes and diagenetic trace-element redistribution at the scale of individual colour-defined domains and sediment components.

3.2.1 Early diagenetic mobilisation of trace elements in marine red carbonates

Marine red beds (MRBs) are carbonate, siliceous or clastic deposits characterised by red colouration due to the presence of iron oxides (Jansa and Hu 2009; Hu et al. 2012;

Bábek et al. 2018). They occur in several stratigraphic intervals across the Phanerozoic, with notable concentrations in the Ordovician, Devonian, Jurassic and Cretaceous, which led to the concept of MRBs as time-specific facies (Brett et al. 2012). The submicron Fe-oxide pigments responsible for the red colour are interpreted as authigenic rather than detrital, based on their fine grain size, homogeneous distribution and occurrence within bioclasts and microbial fabrics (Mamet and Préat 2006). Three main formation mechanisms have been proposed: hematite precipitation at the sediment–water interface under prolonged oxic conditions (Franke and Paul 1980; Hu et al. 2012); oxidation of dissolved Fe^{2+} accumulated during prior anoxic intervals (Song et al. 2017); and microbially mediated Fe precipitation by Fe(II)-oxidising bacteria along redox microgradients (Préat et al. 2006; Mamet and Préat 2006).

A key characteristic of MRBs is strong vertical and lateral colour variability: red, grey, yellow and pink limestones alternate over centimetre to metre scales. The **Papers 11 to 14** address three questions: (i) what mineral phases, microstructures and processes control Fe-oxide precipitation across different paleogeographic settings; (ii) what geochemical contrasts between colour domains are detectable at the microscale but concealed in bulk-rock data; and (iii) can colour stratigraphy serve as a reliable proxy of bottom-water redox fluctuations?

Four areas with Paleozoic red carbonates were investigated: Kinnekulle, Sweden (Middle Ordovician orthoceratite limestone; **Paper 12**); Yichang area, South China (Middle–Upper Ordovician; **Paper 13**); Prague Basin, Czech Republic (Lower Devonian, Daleje–Třebotov Formation; **Paper 11**); and Montagne Noire, southern France (Upper Devonian, Frasnian–Famennian; **Paper 14**) (Fig. 1). The approach combined sedimentology, petrophysics, SEM-EDX, bulk-rock element geochemistry, molybdenum stable isotope systematics and *in situ* LA-ICP-MS. My primary responsibility across all four studies was *in situ* LA-ICP-MS data acquisition, analysis and paleoenvironmental and diagenetic interpretation. In total, 831 spots were analysed across 32 thin sections, covering grey, yellow, pink and red micrite, microspar, cements, skeletal grains, microbial structures, peloids, bioturbation fills and Mn-oxide-rich matrix.

At bulk-rock scale, red facies are enriched in Fe and depleted in U in all four areas (**Papers 11 to 14**); Mo and Cu are depleted in red and enriched in non-red facies in Prague Basin (**Paper 11**), Montagne Noire (**Paper 14**) and South China (**Paper 13**). Bulk-rock ΣREE correlates with Al in all four areas (R^2 0.6–0.98), meaning that bulk Ce and Eu anomalies reflect detrital contamination rather than redox conditions and cannot be used as paleoredox proxies.

In situ data consistently reveal larger geochemical contrasts between colour domains than bulk analyses. Red micrite is enriched in Fe and depleted in U across all areas (Figs. 16 and 17), which is the most robust and regionally consistent signal. In opposite to bulk samples, LA-ICP-MS measurements allow to target on carbonate components, with low detrital contamination and some of them provided seawater-like signal. In the Prague Basin, *in situ* analyses of low-Al carbonate components reveal

Ce/Ce* up to 9 in red micrite and up to 20 in cements, while bulk Ce/Ce* remains near 1 across the entire colour spectrum (**Paper 11**). In the Montagne Noire, both positive and negative Ce anomalies develop progressively from grey to red microspar at the microscale while bulk anomalies remain uniformly weak. Microbial structures (microstromatolites, laminated shell envelopes, microborings and *Frutexites*) consistently show higher and more variable Fe, Mn, V, Mo and U concentrations than surrounding micrite in all areas, recording localised redox conditions invisible in bulk data (Fig. 17; **Paper 14**). In Baltoscandia, grey micrite in burrow fills shows reversed or absent colour-related trends relative to the surrounding red matrix (Fig. 16c), demonstrating that element redistribution occurred at or very close to the sediment–water interface (**Paper 12**).

Fe-oxide precipitation is closely coupled with authigenic clay mineral formation, as evidenced in Montagne Noire (**Paper 14**): submicron hematite occurs exclusively in association with authigenic filamentous and vermicular K–Fe–Mg aluminosilicates, not with their detrital counterparts, within microstromatolites, microborings and ferruginous oncoids containing organic matter and fluorapatite. This spatial association indicates that organomineralization and microbial Fe-oxidizing activity contributed to Fe cycling and trace-element fixation, although abiotic pathways involving Fe^{2+} sorption onto authigenic clay surfaces and subsequent oxidation cannot be excluded. Microbial fabrics represent microscale geochemical hotspots where Fe, Mn and redox-sensitive elements are selectively concentrated, with redox variability operating at sub-millimetre scales exceeding that observable at bulk-rock scale.

The same coupling between authigenic aluminosilicates and submicron hematite was documented in the Lower Devonian Daleje–Třebotov Formation of the Prague Basin, where hematization of detrital Fe–Mg phyllosilicates and microbially mediated precipitation within microstromatolites and oncoids were identified as the principal reddening mechanisms. Negative δ^{98}Mo values in the red facies and positive values in the non-red and black facies support redox control by pore-water reactions rather than Fe enrichment from Fe^{2+}-supersaturated ocean waters, contradicting that model of MRB formation (**Paper 11**).

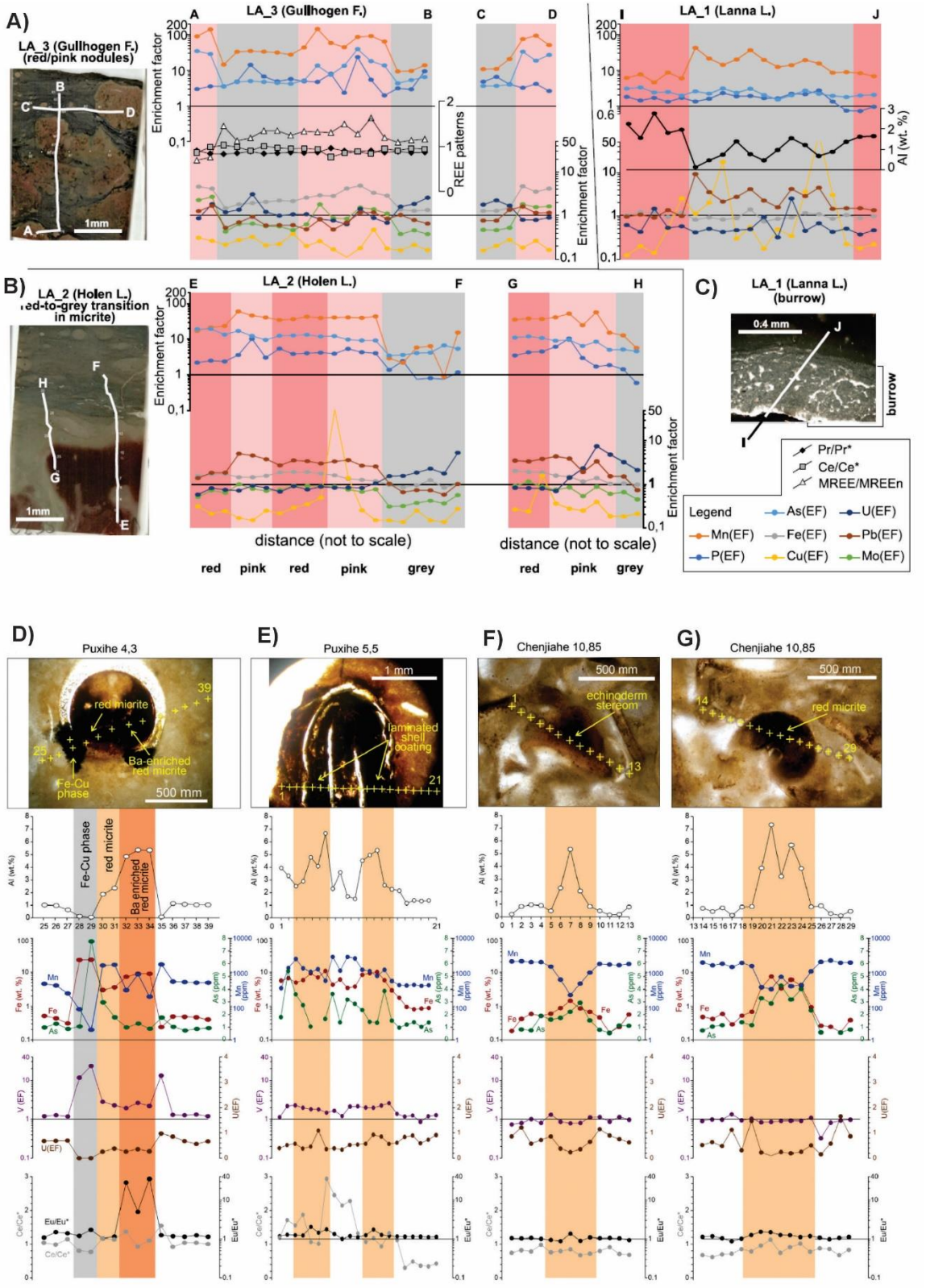
A)
LA_3 (Gullhogen F.)
(red/pink nodules)
LA_3 (Gullhogen F.)
LA_1 (Lanna L.)
Enrichment factor
REE patterns
Al (wt. %)
B)
LA_2 (Holen L.)
red-to-grey transition
in micrite)
LA_2 (Holen L.)
distance (not to scale)
red pink red pink grey
red pink grey
C)
LA_1 (Lanna L.)
(burrow)
0.4 mm
burrow
Pr/Pr*
Ce/Ce*
MREE/MREEn
Legend
As(EF) U(EF)
Mn(EF) Fe(EF) Pb(EF)
P(EF) Cu(EF) Mo(EF)
D)
Puxihe 4,3
red micrite
Ba-enriched red micrite
Fe-Cu phase
500 mm
E)
Puxihe 5,5
1 mm
laminated shell coating
F)
Chenjiahe 10,85
500 mm
echinoderm stereom
G)
Chenjiahe 10,85
500 mm
red micrite
Al (wt.%)
Fe-Cu phase
red micrite
Ba enriched red micrite
Fe (wt. %)
Mn (ppm)
As (ppm)
V (EF)
U(EF)
Ce/Ce*
Eu/Eu*

Figure 16. (A-C) Distribution of LA-ICP-MS geochemical proxies (enrichment factors and REE patterns) along lines crossing various colour and diagenetic features in thin sections from Ordovician of Baltoscandia, (D-G) from south China : (A) pink nodules in grey marl, Gullhögen Formation; (B) red-to-grey transition in micrite, Holen Limestone; (C) burrow filled by grey micrite in red-micrite matrix, Lanna Limestone; (D) PX-4.3 - red micrite in the skeletal interior of orthoconid nautiloids; (E) PX-5.5 - laminated Fe-hydroxide overgrowths of a mollusc skeletal fragment; (F) SH-10.85 - red staining of echinoderm stereom; (G) SH-10.85 - red-stained micrite infill of a gastropod shell.

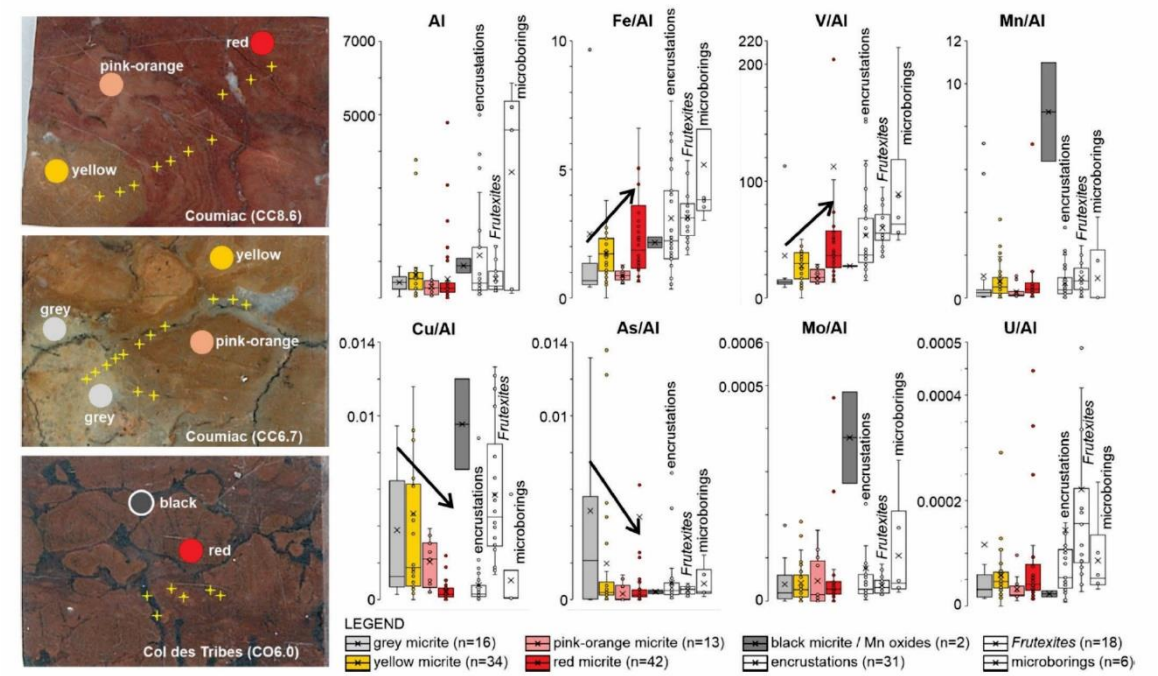

Figure 17. LA-ICP-MS data from various components of the studied thin-sections from the Montagne Noire Frasnian-Famennian boundary sections: (a) polished slabs showing micrite with variable colour: grey, yellow, orange-pink, red and black; (b) boxplots of Al contents and Al-normalized element ratios of the main components — coloured micrite, encrustations on brachiopod shells, *Frutexites* microproblematica, and microborings in brachiopod shells. Far outliers are not shown.

The *in situ* geochemical data from both the Prague Basin (**Paper 11**) and Montagne Noire (**Paper 14**) confirm that the grey-to-red colour transition is systematically accompanied by Fe and V enrichment and U and Cu depletion. This is the elemental shifts predicted by models of redox gradient zonation in the shallow sediment subsurface (Froelich et al. 1979; Algeo and Li 2020): (i) Fe-oxide precipitation zone (red,

oxic), (ii) Fe enrichment zone (grey, suboxic), (iii) U-Mo enrichment zone (grey/green, suboxic) and (iv) Cu-V-Mo enrichment zone (grey/black, suboxic to anoxic). In the Montagne Noire, the same diagenetic hematitization mechanism operated during oxic seafloor conditions, but the red succession is punctuated by eight dark horizons that record bottom-water dysoxia to anoxia of the Late Devonian anoxic events (Kellwasser Crisis, Nehden and Condroz events), demonstrating that MRB colour stratigraphy can serve as a sensitive palaeoceanographic proxy for seafloor redox conditions (**Paper 14**).

In summary, colour variability in MRBs operates at two distinct scales: micro- to centimetre-scale mottling and discrete domains (e.g., microbial structures, borrows, infills; Figs. 16 and 17) reflect *in situ* diagenetic Fe redistribution, whereas decimetre to metre-scale patterns record either diagenetic zonation or bottom-water redox fluctuations. The distinction between these scales is therefore critical for any palaeoenvironmental interpretation. MRBs thus represent a complex archive in which bottom-water oxygenation, sedimentation rate, organic matter input and diagenesis leave superimposed and potentially overprinting signals. Their interpretation requires integration of sedimentological, petrographic and microgeochemical data, with careful discrimination between local diagenetic overprints and broader palaeoenvironmental trends.

3.2.2 Geochemical Insights into Formation of Lower Devonian Ferruginous Oncolites

The preceding studies on MRB illustrated the central role of Fe-Mn redox cycling at and below the sediment-water interface in controlling carbonate geochemistry at the microscale, usually related with microbial activity. A natural extension of this work is to examine Fe biogeochemical cycling at even higher resolution at scale of individual laminae within a single grain. Microstromatolitic envelopes, cortoids and oncoids observed during the MRB studies illustrated how specific microbial consortia concentrated Fe and trace elements, but the laminae of these structures are typically thinner than the LA-ICP-MS laser spot diameter, preventing analysis of individual laminar increments. The ferruginous oncoids from red limestones of the Lower Devonian Praha Formation, Prague Basin, Czechia (Fig. 1) represent a unique exception: their cortical laminae of alternating hematite, chamosite and iron-bearing calcite reach thicknesses resolvable by *in situ* analysis, enabling a direct geochemical record of individual Fe-cycling episodes within a single grain at the level of individual laminas (Fig. 18; **Paper 15**).

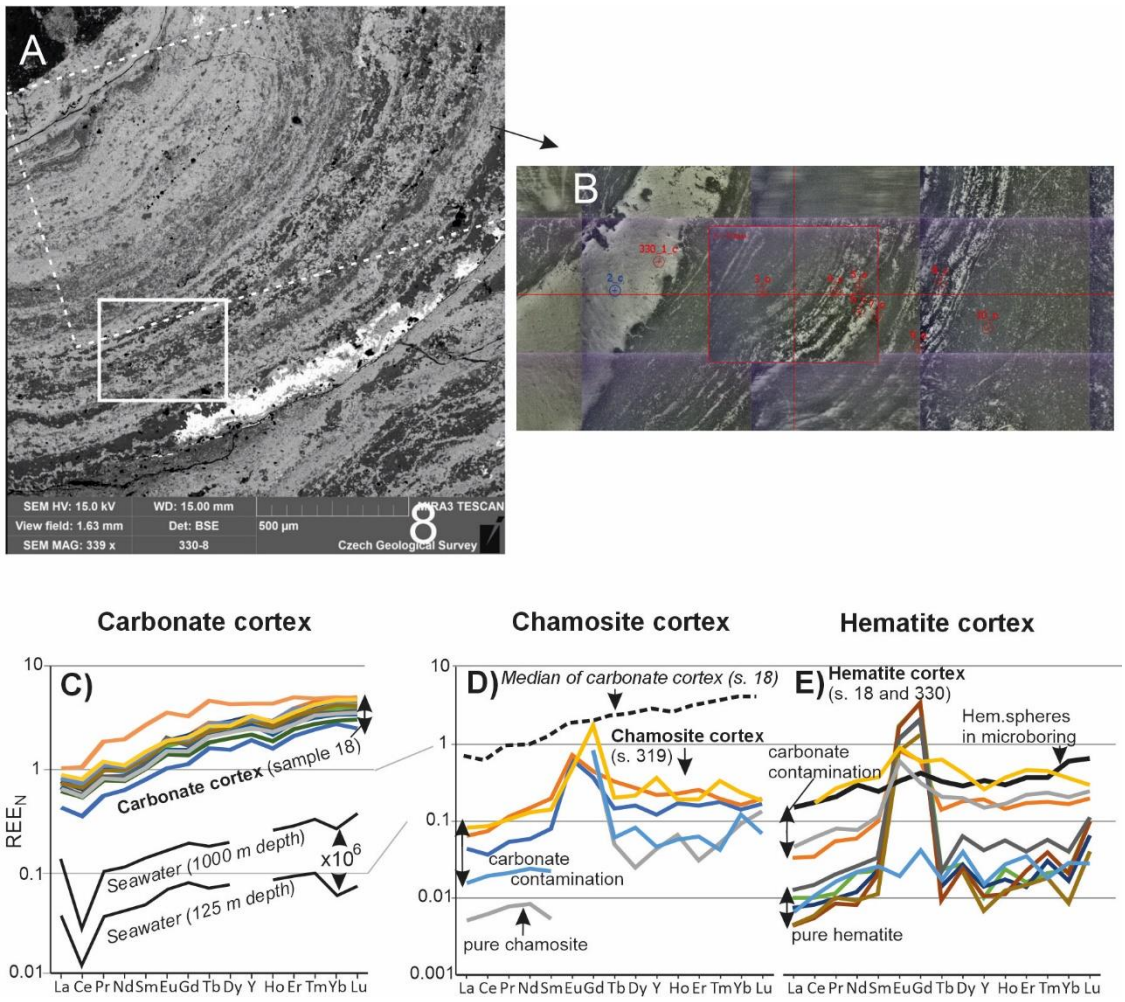

Figure 18. (A) BSE image of features of the oncoidal ironstone interval from the uppermost part of the Řeporyje Limestone, Stydlé Vody Quarry. (B) reflected light image from imaging of LA-ICP-MS system with some of the measured spots; (C-E) UCC-normalized REE patterns of selected components of the studied oncolites. (C) Carbonate cortical laminae (multicoloured curves, sample 18) and modern seawater (black curves; Deng et al., 2017); seawater values increased by 7 orders of magnitude for scaling. (D) Chamosite cortical laminae with varying degrees of carbonate and hematite contamination (multicoloured curves); median of carbonate cortical laminae from sample 18 (black dashed curve) shown for comparison. (E) Hematite cortical laminae with varying degrees of carbonate contamination (multicoloured curves) and hematite spheres in microborings (black curve).

The Řeporyje Limestone at the Stydlé Vody Quarry was deposited in offshore conditions below storm wave base, within red bioturbated skeletal wacke-packstones. Two ironstone horizons were sampled, both forming lenticular bodies ~30 cm thick with positive topographic relief, composed of oncoids, cortoids and ooids. The study

integrated bulk XRD mineralogy, thin-section and outcrop petrography, SEM-EDS and *in situ* LA-ICP-MS. My primary responsibility was LA-ICP-MS data acquisition, processing and geochemical interpretation. I carried out a component-by-component analysis of carbonate nuclei, three cortical laminae types (Fe-calcite, hematite, chamosite), hematitised silicate matrix, carbonate matrix, microborings and calcite veins.

The *in situ* LA-ICP-MS data reveal large geochemical contrasts between individual components that are directly interpretable in terms of Fe-cycling processes. Carbonate nuclei have the lowest Fe and highest $CaCO_3$; cortical Fe-calcite contains ~14 wt% Fe; chamosite laminae ~50 wt% Fe; and hematite laminae ~52–64 wt% Fe. Cortical iron-bearing calcite with the best-preserved signal shows Mn/Sr <1.5, excluding significant meteoric diagenetic overprint, and REE characteristics that are hydrogenous-like: LREE < MREE < HREE pattern, negative Ce anomaly (0.72–0.78), positive Y and Gd anomalies - consistent with suboxic precipitation conditions (Fig. 18c). Pure hematite laminae show very low REE contents, strong positive Eu anomalies (39.8–106.7) and weak or absent Ce anomalies (Fig. 18e), inconsistent with hydrogenous origin and pointing to hydrothermal influence, confirmed by multiple independent proxies: Al/(Al+Fe+Mn) vs. Fe/Ti plots (Fig. 19a) fall in the metalliferous sediments field (Boström 1973), total REE content (La+Ce+Sm+Nd+Eu+Tb+Yb+Lu) *vs*. Cu+Co+Ni diagram (Fig. 19b) shows spots in field characteristic of hydrothermal (Dymek and Klein 1988), and Ce/Ce* *vs.* Nd diagram (Fig. 19c) for discrimination of the origin of marine Fe–Mn (oxyhydr)oxides (Bau et al., 2014) reveals the hydrothermal signature as well. The Eu/Sm vs. Sm/Yb mixing diagram (Fig. 19e) indicates <1–5% hydrothermal fluid contribution, consistent with episodic low-flux venting of diluted Fe^{2+}-bearing fluids mixing with oxygenated seawater at the sediment–water interface (Alexander et al. 2008).

The microbial origin of the oncoids is supported by internal fabric, mineral associations, and geochemical signatures. The cortex lamination is irregular, wavy, and shows a high degree of inheritance, flexure, and overgrowth of surface irregularities, including microdomal structures, which are consistent with growth within cohesive microbial mats. Additional evidence is provided by the presence of encrusting foraminifers, which likely utilized the oncoids as both a substrate and a food source linked to microbial consortia. Indirect indicators include microborings with hematite microspheres and the intimate association of Fe-bearing mineral phases reflecting microbially mediated redox cycling. Furthermore, elevated REE concentrations and seawater-like REE patterns observed in the oncoidal cortices (Fig. 18c) support precipitation from seawater modified within microbially influenced microenvironments, consistent with organomineralization processes.

The occurrence of ironstone lenses is restricted to Stydlé Vody with no coeval equivalents elsewhere in the Prague Basin. This is incompatible with regional iron sources such as continental weathering or basin-wide anoxic events, which would produce laterally continuous ironstone horizons. Hydrothermal venting via the Tachlovice

fault system is the most probable source of Fe, supported by the REE and trace element signatures of hematite, by metasomatic mineral associations restricted to ironstone bodies, by proximity to Lower Devonian mud-mounds commonly interpreted as hydrothermally influenced structures (Belka 1998; Aitken et al. 2002), and by late Silurian to Early Devonian volcanic activity in the Prague Basin (Tasáryová et al. 2018) providing the thermal gradient for hydrothermal fluid circulation.

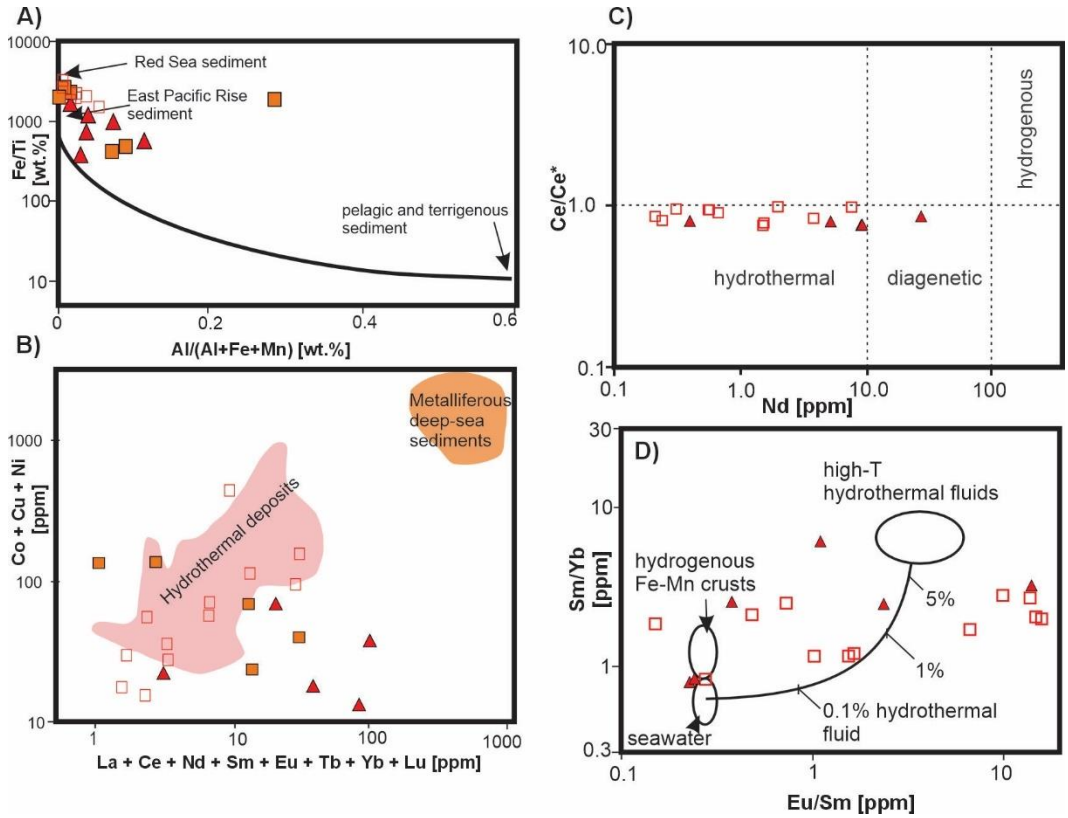

Figure 19. (**a**) Al/(Al+Fe+Mn) vs. Fe/Ti diagram (modified after Boström, 1973) showing mixing between metalliferous and terrigenous sediments. (**b**) Total REE content (La+Ce+Sm+Nd+Eu+Tb+Yb+Lu) vs. Cu+Co+Ni diagram showing fields characteristic of hydrothermal and metalliferous sediments (after Dymek and Klein, 1988). (**c**) Ce/Ce* vs. Nd diagram for discrimination of the origin of marine Fe–Mn (oxyhydr)oxides (after Bau et al., 2014). (**d**) Two-component conservative mixing diagram for Sm/Yb and Eu/Sm (Alexander et al. 2008), showing that a high-temperature hydrothermal fluid contribution of less than 1% is sufficient to produce ratios observed in most hematite laminae, and 1–5% for one spot in hematitized matrix. Note that only hematite and hematitized matrix are plotted, as the diagram is intended for Fe–Mn (oxyhydr)oxides.

The lamina-scale alternation of hematite, chamosite and iron-bearing calcite reflects repeated switches between oxidising and reducing microenvironments within the mat, most plausibly driven by coupled microbial oxidation and reduction: episodic

hydrothermal Fe^{2+} supply mixes with oxic seawater at the sediment–water interface, creating opposing Fe^{2+}/O_2 gradients where microaerophilic Fe-oxidising bacteria compete with chemical oxidation; the resulting bacteriogenic ferrihydrite serves as substrate for Fe-reducing bacteria in anoxic mat zones; and the chamosite precursor forms through passive microbial authigenesis (Fig. 20). Neither microbial cells nor biomarkers were preserved, however, and abiotic Fe-oxide precipitation within pre-existing porous microbial structures cannot be excluded. Both probably operated together, consistently with the interpretation of MRBs in **Papers 11 to 14**.

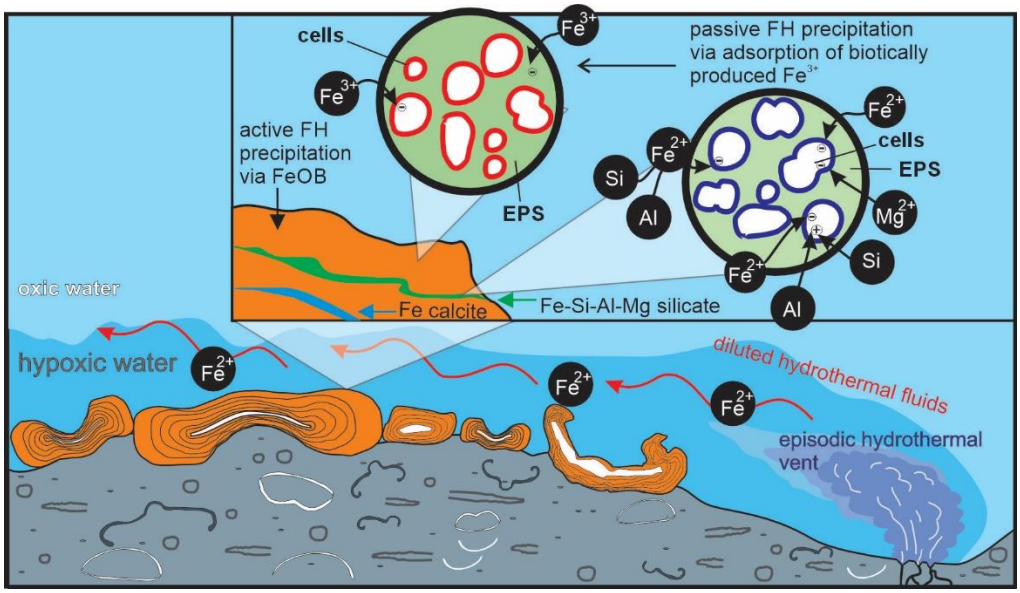

Figure 20. Hypothetized model of oncoid formation.

3.2.3 Conclusive remarks

Marine red beds represent a recurrent Phanerozoic facies whose formation mechanisms and paleoenvironmental significance have long been debated. Across Papers 11–14, my primary contribution was *in situ* LA-ICP-MS microanalysis, which consistently revealed geochemical contrasts between colour domains orders of magnitude larger than those detectable in bulk-rock data, and demonstrated that bulk REE systematics including Ce anomalies are dominated by detrital contamination and cannot serve as paleoredox proxies. A coherent multi-scale diagenetic framework emerged from this work, ranging from a four-zone subsurface redox model in the Prague Basin to stratigraphic-scale bottom-water fluctuation modes in the Montagne Noire, with microbial microenvironments identified as geochemical hotspots coupling Fe-oxide precipitation with authigenic clay formation. I have extended this microgeochemical approach to an even finer scale, resolving individual laminae within ferruginous oncoids of the

Lower Devonian Praha Formation, where component-by-component LA-ICP-MS analysis revealed suboxic bicohemical precipitation recorded in cortical Fe-calcite and episodic hydrothermal Fe^{2+} input evidenced by anomalous Eu enrichment in pure hematite laminae. Taken together, these studies position *in situ* LA-ICP-MS microgeochemistry as the indispensable methodological bridge between sedimentary fabric observation and paleoenvironmental reconstruction in Paleozoic iron-rich marine carbonates. This demonstrates the complexity of Fe biogeochemical cycling in oxidizing marine systems, which is only accessible below the resolution of conventional bulk analysis.

4 Conclusions and Outlook

This Habilitation thesis synthesises ten years of my research in the field of Paleozoic stratigraphy and paleoenvironmental reconstructions. Across its four topics, the work addresses two interconnected challenges in the geosciences: how to establish reliable time control in deep-time records, and how to extract meaningful paleoenvironmental signals from those archives.

The stratigraphic contributions (Topics A and B) have direct implications for the global geological timescale. The testing of the Montpellier Criteria for redefining the DCB demonstrated that the combination of the Zr/Al detrital proxy and the base of the *Protognathodus kockeli* conodont Zone provides a reproducible, multi-criteria boundary level across contrasting depositional settings on two continents. This represents a step towards resolving a problem that was open for nearly five decades. These results have been recognised through my involvement as a voting member of the Devonian-Carboniferous GSSP Reappraisal Task Group under the International Commission on Stratigraphy. The lower Tournaisian research established an integrated biostratigraphic and chemostratigraphic framework that improves interregional correlation and connects isolated regional zonation schemes.

The paleoenvironmental research (Topics C and D) demonstrates the power and necessity of combining multiple geochemical proxies across scales. My Hangenberg Crisis studies show that marine anoxia at the DCB was driven by the interplay of continental runoff, volcanic and hydrothermal nutrient input, and progressive basin restriction, mechanisms whose relative importance varied spatially and temporally. The marine red beds studies reveal that colour variability in Paleozoic iron-rich carbonates reflects the superposition of processes at fundamentally different scales: micro- to centimetre-scale mottling records *in situ* diagenetic redistribution within the sediment, while decimetre-to-metre-scale patterns track bottom-water redox fluctuations on geological timescales. Microbial microenvironments emerge as the principal locus of Fe-oxide precipitation and trace-element fixation, coupling Fe cycling with authigenic clay formation in ways invisible to bulk analysis.

Methodologically, the second part of the thesis traces a progression from bulk geochemistry towards increasingly high-resolution *in situ* microanalysis. LA-ICP-MS targeted at individual microfabric components has become the principal analytical tool of my research. Signals that are averaged at the bulk scale become interpretable at the scale of laminae, colour domains, or individual cortical layers in oncoids. This methodological trajectory will continue, with framboidal pyrite geochemistry and multi-proxy redox reconstruction in carbonate-dominated successions representing the next frontier.

The research I describe in this thesis is continuing in several directions. In stratigraphy, along with DCB task, I am currently focusing on the Early Devonian Daleje Event

in the Prague Basin within the Czech Science Foundation project *Chronostratigraphic and Paleoenvironmental Analysis of the Daleje Event in its type area: Implications for the Emsian (Early Devonian) Subdivision*, and on the lower Famennian and middle-upper Tournaisian, extending the integrated biostratigraphic and chemostratigraphic approach developed here to these less well-constrained intervals. Methodologically, the approach is expanding towards framboidal pyrite and electron microprobe analysis as additional redox proxies, with growing emphasis on distinguishing microbial from abiotic precipitation pathways and their respective geochemical signatures in carbonate and other sedimentary archives. Beyond the Palaeozoic, I apply the same approach to Mesozoic archives. I study Jurassic microbial carbonates and Cretaceous glauconites, where the same questions about microbial versus abiotic precipitation and diagenetic overprint come in different paleoenvironmental and geologic context. These topics are being developed and explored also through PhD and Master's projects currently running in my group. This helps to open questions and test what each approach in specific way of signal preservation can realistically contribute, while transferring knowledge and skills through the research and student projects I supervise, as well as in the courses I teach (sedimentology, historical geology).

Bibliography

Publications by the author not included among annotated Papers 1–15

Hartenfels, S., Becker, R. T., Herbig, H.-G., Qie, W., **Kumpan, T.**, De Vleeschouwer, D., Weyer, D., Kalvoda, J., & (2022). The Devonian-Carboniferous transition at Borkewehr near Wocklum (northern Rhenish Massif, Germany) - a potential GSSP section. *Palaeobiodiversity and Palaeoenvironments*, 102, 763–829.

Kalvoda, J., & **Kumpan, T.** (2021). Lower Tournaisian microbialite-rich facies at the Mokrá quarries, Czech Republic. *Acta Musei Moraviae, Scientiae Geologicae*, 106, 171–180.

Kumpan, T., Bábek, O., Frýda, J., & Šimíček, D. (2018). Hranice mezi devonem a karbonem v západním Utahu (Confusion Range, Burbank Hills). In M. Faměra, K. Kropáč, D. Šimíček, & T. Lehotský (Eds.), Paleozoikum 2018: Sborník abstraktů, XXI. ročník (s. 8). Univerzita Palackého v Olomouci, Přírodovědecká fakulta, Katedra geologie.

Kumpan, T., Bábek, O., Kalvoda, J., Frýda, J., & Matys Grygar, T. (2014a). A high-resolution, multiproxy stratigraphic analysis of the Devonian–Carboniferous boundary sections in the Moravian Karst (Czech Republic) and a correlation with the Carnic Alps (Austria). *Geological Magazine*, 151, 201–215.

Kumpan, T., Bábek, O., Kalvoda, J., Matys Grygar, T., & Frýda, J. (2014b). Sea-level and environmental changes around the Devonian–Carboniferous boundary in the Namur–Dinant Basin (S Belgium, NE France): a multi-proxy stratigraphic analysis of carbonate ramp archives and its use in regional and interregional correlations. *Sedimentary Geology*, 311, 43–59.

Kumpan, T., Bábek, O., Kalvoda, J., Matys Grygar, T., Frýda, J., Becker, R. T., & Hartenfels, S. (2015). Petrophysical and geochemical signature of the Hangenberg Events: an integrated stratigraphy of the Devonian-Carboniferous boundary interval in the Northern Rhenish Massif (Avalonia, Germany). *Bulletin of Geosciences*, 90, 667–694.

Spalletta, C., Corradini, C., Feist, R., Korn, D., **Kumpan, T.,** Perri, M. C., Pondrelli, M., & Venturini, C. (2021) The Devonian–Carboniferous boundary in the Carnic Alps (Austria and Italy). *Palaeobiodiversity and Palaeoenvironments*, 101, 487–505.

Vodrážková, S., Koubová, M., Munnecke, A., **Kumpan, T.,** Vodrážka, R., Pour, O. & Frýda, J. 2025. Clay mineral authigenesis as an example of organomineralization in Paleozoic coated grains and peloids. *Sedimentary Geology*, 484, Article 106912.

Other references

Aitken, S. A., Henderson, C. M., Collom, C. J., Johnston, P. A. (2002). Stratigraphy, paleoecology, and origin of Lower Devonian (Emsian) carbonate mud buildups, Hamar Laghdad, eastern Anti-Atlas, Morocco, Africa. Bulletin of Canadian Petroleum Geology, 50, 217–243.

Alberti, H., Groos-Uffenorde, H., Streel, M., Uffenorde, H., & Walliser, O. H. (1974). The stratigraphical significance of the Protognathodus fauna from Stockum (Devonian/Carboniferous boundary, Rhenish Schiefergebirge). Newsletters on Stratigraphy, 3, 263–276.

Alexander, W. B., Bau, M., Andersson, P., & Dulski, P. (2008). Continentally-derived solutes in shallow Archean seawater: rare earth element and Nd isotope evidence in iron formation from the 2.9 Ga Pongola Supergroup, South Africa. Geochimica et Cosmochimica Acta, 72, 378–394.

Algeo, T. J., & Scheckler, S. E. (1998). Terrestrial-marine teleconnections in the Devonian: links between the evolution of land plants, weathering processes, and marine anoxic events. Philosophical Transactions of the Royal Society of London B: Biological Sciences, 353, 113–130.

Algeo, T., Lyons, T. W., Blakey, R. C., & Over, J. D. (2007). Hydrographic conditions of the Devono–Carboniferous North American seaway inferred from sedimentary Mo–TOC relationships. Palaeogeography, Palaeoclimatology, Palaeoecology, 256, 204–230.

Algeo, T. J., & Li, C. (2020). Redox classification and calibration of redox thresholds in sedimentary systems. Geochimica et Cosmochimica Acta, 287, 8–26.

Algeo, T. J., & Liu, J. (2020). A re-assessment of elemental proxies for paleoredox analysis. Chemical Geology, 540, 119549.

Algeo, T. J., & Tribovillard, N. (2009). Environmental analysis of paleoceanographic systems based on molybdenum–uranium covariation. Chemical Geology, 268, 211–225.

Aretz, M., & Corradini, C. (2019). The redefinition of the base of the Carboniferous Period. 19th International Congress on the Carboniferous and Permian (XIX ICCP 2019), 10, 10.

Aretz, M., & Corradini, C. (2021). Global review of the Devonian-Carboniferous boundary: an introduction. Palaeobiodiversity and Palaeoenvironments, 101, 285–293.

Aretz, M., Herbig, H.G., Wang, X.D., Gradstein, F.M., Agterberg, F.P. & Ogg, J.G., 2020. The Carboniferous Period. In: Gradstein, F.M., Ogg, J.G., Schmitz, M.D., Ogg, G.M. (Eds.), Geologic Time Scale 2020, Vol. 2. Elsevier, pp. 811–874.

Bábek, O., Faměra, M., Hladil, J., Kapusta, J., Weinerová, H., Šimíček, D., Slavík, L., & Ďurišová, J. (2018). Origin of red pelagic carbonates as an interplay of global climate and local basin factors: insight from the Lower Devonian of the Prague Basin, Czech Republic. Sedimentary Geology, 364, 71–88.

Bardasheva, N. P., Bardashev, I. A., Weddige, K., & Ziegler, W. (2004). Stratigraphy and conodonts of the Lower Carboniferous of the Shishkat section (southern Tien Shan, Tajikistan). Senckenbergiana Lethaea, 84, 225–301.

Bau, M. (1991). Rare earth element mobility during hydrothermal and metamorphic fluid–rock interaction and the significance of the oxidation state of europium. Chemical Geology, 93, 219–230.

Bau, M., & Dulski, P. (1996). Distribution of yttrium and rare-earth elements in the Penge and Kuruman iron-formations, Transvaal Supergroup, South Africa. Precambrian Research, 79, 37–55.

Bau, M., Schmidt, K., Koschinsky, A., Hein, J., Kuhn, T., & Usui, A. (2014). Discriminating between different genetic types of marine ferro-manganese crusts and nodules based on rare earth elements and yttrium. Chemical Geology, 381, 1–9.

Becker, R. T. (1993). Analysis of ammonoid palaeobiogeography in relation to the global Hangenberg (terminal Devonian) and Lower Alum Shale (Middle Tournaisian) events. Annales de la Société Géologique de Belgique, 115, 459–473.

Becker, R. T., Hartenfels, S., & Kaiser, S. I. (2021). Review of Devonian-Carboniferous Boundary sections in the Rhenish Slate Mountains (Germany). Palaeobiodiversity and Palaeoenvironments, 101, 357–420.

Becker, R. T., Kaiser, A. I., & Aretz, M. (2016). Review of the chrono-, litho- and biostratigraphy across the global Hangenberg Crisis and Devonian-Carboniferous Boundary. Geological Society, London, Special Publications, 423, 355–386.

Becker, R.T., Marshall, J.E.A., Da Silva, A.-C., Agterberg, F.P., Gradstein, F.M., Ogg, J.G., 2020. The Devonian Period. In: Gradstein, F.M., Ogg, J.G., Schmitz, M.D., Ogg, G.M. (Eds.), Geologic Time Scale 2020, Vol. 2. Elsevier, pp. 733–810.

Belka, Z. (1998). Early Devonian Kess-Kess carbonate mud mounds of the eastern Anti-Atlas (Morocco), and their relation to submarine hydrothermal venting. Journal of Sedimentary Research, 68, 368–377.

Bischoff, G. (1957). Die Conodonten-Stratigraphie des rhenoherzynischen Unterkarbons mit Berücksichtigung der Wocklumeria-Stufe und der Devon/Karbon-Grenze. Abhandlungen des Hessischen Landesamtes für Bodenforschung, 19, 1–64.

Blakey, R. (2012). Global Paleogeography. Colorado Plateau Geosystems, Inc.

Boström, K. (1973). The origin and fate of ferromanganoan active ridge sediments. Stockholm contributions in geology. Acta Universitatis Stockholmensis, 27, 149–243.

Boström, K. (1983). Genesis of ferromanganese deposits—diagnostic criteria for recent and old deposits. Hydrothermal Processes at Seafloor Spreading Centers, 473, 473–489.

Bouckaert, J. & Groessens, E., 1976. Polygnathus paprothae, Pseudopolygnathus conili, Pseudopolygnathus graulichi: espèces nouvelles à la limite Dévonien–Carbonifère. Annales de la Société Géologique de Belgique 99, 587–599.

Branson, E. B., & Mehl, M. G. (1934). Conodonts from the Grassy Creek Shale of Missouri. University of Missouri Studies, 8, 171–259.

Brett, C. E., McLaughlin, P. I., Histon, K., Schindler, E., & Ferretti, A. (2012). Time-specific aspects of facies: state of the art, examples, and possible causes. Palaeogeography, Palaeoclimatology, Palaeoecology, 367, 6–18.

Buggisch, W., Joachimski, M. M., Sevastopulo, G., & Morrow, J. R. (2008). Mississippian δ^{13}C_carb and conodont apatite δ^{18}O records — their relation to the Late Palaeozoic Glaciation. Palaeogeography, Palaeoclimatology, Palaeoecology, 268, 273–292.

Caplan, M. L., & Bustin, R. M. (1999). Devonian-Carboniferous Hangenberg mass extinction event, widespread organic-rich mudrock and anoxia: causes and consequences. Palaeogeography, Palaeoclimatology, Palaeoecology, 148, 187–207.

Carmichael, S. K., Waters, J. A., Batchelor, C. J., Coleman, D. M., Suttner, T. J., Kido, E., Moore, L. M., & Chadimová, L. (2016). Climate instability and tipping points in the Late Devonian: detection of the Hangenberg Event in an open oceanic island arc in the Central Asian Orogenic Belt. Gondwana Research, 32, 213–231.

Chlupáč, I., Jaeger, H. & Zikmundová, J. 1972. The Silurian-Devonian boundary in the Barrandian. Bulletin of the Canadian Petroleum Geology, 20(1), 104–174.

Cole, D., Myrow, P.M., Fike, D.A., Hakim, A. & Gehrels, G.E. (2015). Uppermost Devonian (Famennian) to Lower Mississippian events of the western U.S.: Stratigraphy, sedimentology, chemostratigraphy, and detrital zircon geochronology. Palaeogeography, Palaeoclimatology, Palaeoecology, 427, 1–19.

Conil, R., Dreesen, R., Lentz, M.A., Lys, M. & Plodowski, G., 1986. The Devono-Carboniferous transition in the Franco-Belgian basin with reference to Foraminifera and brachiopods. Annales de la Société Géologique de Belgique 109 (1), 19–26.

Conybeare, W. D., & Phillips, W. (1822). Outlines of the geology of England and Wales. London.

Corradini, C., Kaiser, S. I., Perri, M. C., & Spalleta, C. (2011). Protognathodus (Conodonta) and its potential as a tool for defining the Devonian/Carboniferous boundary. Rivista Italiana di Paleontologia e Stratigrafia, 117, 15–28.

Corradini, C., Schönlaub, H. P., & Kaiser, S. I. (2017). The Devonian/Carboniferous boundary in the Grüne Schneid section. International Conodont Symposium 4, Valencia, 271, 271–275.

Cowie, J.W., Ziegler, W., Boucot, A.J., Bassett, M.G. & Remane, J. (1986): Guidelines and statutes of the International Commission on Stratigraphy (ICS). Courier Forschungsinstitut Senckenberg, 83, 1–14.Craigie, N. (2018). Principles of elemental chemostratigraphy. Springer.

Cramer, B. D., & Jarvis, I. 2020) Carbon isotope stratigraphy. In: Gradstein, F.M., Ogg, J.G., Schmitz, M.D., Ogg, G.M. (Eds.), Geologic Time Scale 2020, Vol. 2. Elsevier, pp. 309–343).

Della Porta, G., Webb, G. E., & McDonald, I. (2015). REE patterns of microbial carbonate and cements from Sinemurian (Lower Jurassic) siliceous sponge mounds (Djebel Bou Dahar, High Atlas, Morocco). Chemical Geology, 400, 65–86.

Denayer, J., Prestianni, C., Mottequin, B., Hance, L., & Poty, E. (2021). The Devonian–Carboniferous boundary in Belgium and surrounding areas. Palaeobiodiversity and Palaeoenvironments, 101, 313–356.

Dymek, R. F., & Klein, C. (1988). Chemistry, petrology, and origin of banded iron-formation lithologies from the 3800 Ma Isua Supracrustal Belt, West Greenland. Precambrian Research, 39, 247–302.

Ebner, F. (1978). Stratigraphie des Karbon der Rannachfazies im Paläozoikum von Graz, Österreich. Mitteilungen der Österreichischen Geologischen Gesellschaft, 69, 163–196.

Elderfield, H., Upstill-Goddard, R., & Sholkovitz, E. R. (1990). The rare earth elements in rivers, estuaries, and coastal seas and their significance to the composition of ocean waters. Geochimica et Cosmochimica Acta, 54, 971–991.

Feist, R., & Petersen, J. 1995. Origin and spread of Pudoproetus, a survivor of the Late Devonian trilobite crisis. Journal of Paleontology, 69(1), 99–109.

Feist, R., Cornée, J. J., Corradini, C., et al. (2021). The Devonian–Carboniferous boundary in the stratotype area (SE Montagne Noire, France). Palaeobiodiversity and Palaeoenvironments, 101, 295–311.

Fields, B. D., Melott, A. L., Ellis, J., Ertel, A. F., Fry, B. J., Lieberman, B. S., Liu, Z., Miller, J. A., & Thomas, B. C. (2020). Supernova triggers for end-Devonian extinctions. Proceedings of the National Academy of Sciences, 117, 21008–21010.

Flajs, G., & Feist, R. (1988). Index conodonts, trilobites and environment of the Devonian-Carboniferous boundary at La Serre (Montagne Noire, France). Courier Forschungsinstitut Senckenberg, 100, 53–107.

Franke, W., & Paul, J. (1980). Pelagic redbeds in the Devonian of Germany: deposition and diagenesis. Sedimentary Geology, 25, 231–256.

Froelich, P., Klinkhammer, G. P., Bender, M. L., Luedtke, N. A., Heath, G. R., Cullen, D., Dauphin, P., Hammond, D., Hartman, B., & Maynard, V. (1979) Early oxidation of organic matter in pelagic sediments of the eastern equatorial Atlantic: suboxic diagenesis. Geochimica et Cosmochimica Acta 43, 1075–1090.

Gradstein, F. M., Ogg, J. G., Schmitz, M. D., & Ogg, G. M. (2020). Geologic Time Scale 2020. Elsevier.

Hass, W. H. (1959). Conodonts from the Chappel Limestone of Texas. U.S. Geological Survey Professional Paper, 294, 385–399.

Hedhli, M., Grasby, S. E., Henderson, C. M., & Davis, B. J. (2023). Multiple diachronous "Black Seas" mimic global ocean anoxia during the latest Devonian. Geology, 51, 973–977.

Hogancamp, N. J., Stolfus, B. M., Cramer, B. D., & Day, J. E. (2019). A revised conodont zonation of the Tournaisian (Kinderhookian to lower Osagean) and implications for stratigraphic correlations in North America. Iowa Geological Survey Guidebook, 30, 11–18.

Hu, X., Scott, R. W., Cai, Y., Wang, C., & Melinte-Dobrinescu, M. C. (2012). Cretaceous oceanic red beds (CORBs): different time scales and models of origin. Earth-Science Reviews, 115, 217–248.

Isaacson, P., Díaz-Martínez, E., Grader, G. W., Kalvoda, J., Bábek, O., & Devuyst, F. X. (2008). Late Devonian–earliest Mississippian glaciation in Gondwanaland and its biogeographic consequences. Palaeogeography, Palaeoclimatology, Palaeoecology, 268, 126–142.

Jansa, L., & Hu, X. (2009). An overview of the Cretaceous pelagic black shales and red beds: origin, paleoclimate and paleoceanographic implications. SEPM Special Publication, 91, 59–72.

Janoušek, V., Aichler, J., Hanžl, P., Gerdes, A., Erban, V., Pecina, V., Žáček, V., Pudilová, M., Hrdličková, K., Mixa, P., & Žáčková, E. (2014). Constraining genesis and geotectonic setting of metavolcanic complexes: a multidisciplinary study of the Devonian Vrbno Group (Hrubý Jeseník Mts., Czech Republic). International Journal of Earth Sciences, 103, 455–483.

Ji, Q. (1985). Study on the phylogeny, taxonomy, zonation and biofacies of Siphonodella (Conodonta). Bulletin of the Institute of Geology, Chinese Academy of Geological Sciences, 11, 51–75.

Ji, Q., & Ziegler, W. (1992). Phylogeny, speciation and zonation of Siphonodella of shallow water facies (Conodonta, Early Carboniferous). Courier Forschungsinstitut Senckenberg, 154, 223–251.

Jongmans, W. J. (1938). Compte rendu du deuxième congrès pour l'avancement des études de stratigraphie carbonifère. Geological Magazine, 75, 90–91.

Kaiser, S. I. (2009). The Devonian/Carboniferous boundary stratotype section (La Serre, France) revisited. Newsletters on Stratigraphy, 43, 195–205.

Kaiser, S. I., & Corradini, C. (2011). The early siphonodellids (Conodonta, Late Devonian–Early Carboniferous): overview and taxonomic state. Neues Jahrbuch für Geologie und Paläontologie, Abhandlungen, 261, 19–35.

Kaiser, S. I., Aretz, M., & Becker, R. T. (2015). The global Hangenberg Crisis (Devonian–Carboniferous transition): review of a first-order mass extinction. Geological Society, London, Special Publications, 423, 387–437.

Kaiser, S. I., Becker, R. T., Spalletta, C., & Steuber, T. (2009). High-resolution conodont stratigraphy, biofacies and extinctions around the Hangenberg Event in pelagic successions from Austria, Italy and France. Palaeontographica Americana, 63, 97–139.

Kaiser, S. I., Steuber, T., & Becker, T. R. (2008). Environmental change during the late Famennian and early Tournaisian (Late Devonian–Early Carboniferous): implications from stable isotopes and conodont biofacies in southern Europe. Geological Journal, 43, 241–260.

Kaiser, S. I., Steuber, T., Becker, T. R., & Joachimski, M. M. (2006). Geochemical evidence for major environmental change at the Devonian–Carboniferous boundary in the Carnic Alps and the Rhenish Massif. Palaeogeography, Palaeoclimatology, Palaeoecology, 240, 146–160.

Kalvoda, J., & Kukal, Z. (1987). Devonian–Carboniferous boundary in the Moravian Karst at the Lesní lom Quarry, Brno-Líšeň, Czechoslovakia. Courier Forschungsinstitut Senckenberg, 98, 95–117.

Kulagina, E. I., Vevel, Y. A., Stepanova, T. I., & Zaytseva, E. L. (2016). Foraminifers of the genus Tournayellina. Paleontological Journal, 50, 557–572.

Lakin, J. A., Marshall, J. E. A., Troth, I., & Harding, I. C. (2016). Greenhouse to icehouse: a biostratigraphic review of latest Devonian–Mississippian glaciations and their global effects. Geological Society, London, Special Publications, 423, 439–464.

Li, F., Yan, J. X., Burne, R. V., Chen, Z. Q., Algeo, T. J., Zhang, W., Tian, L., Gan, Y. L., Liu, K., & Xie, S. C. (2017). Paleo-seawater REE compositions and microbial signatures preserved in laminae of lower Triassic ooids. Palaeogeography, Palaeoclimatology, Palaeoecology, 486, 96–107.

Liu, Y. Q., Ji, Q., Kuang, H. W., Jiang, X. J., Xu, H., & Peng, N. (2012). U-Pb zircon age, sedimentary facies, and sequence stratigraphy of the Devonian-Carboniferous boundary, Daposhang section, Guizhou, China. Palaeoworld, 21, 100–107.

Malá, T. (2020). Revision of the conodont fauna from the Devonian/Carboniferous boundary interval in the Marble quarry at Křtiny. Bachelor's thesis, Masaryk University.

Mamet, B., & Preat, A. (2006). Iron-bacterial mediation in Phanerozoic red limestones: state of the art. Sedimentary Geology, 185, 147–157.

Marshall, J. E. A., Lakin, J., Troth, I., & Wallace-Johnson, S. M. (2020). UV-B radiation was the Devonian-Carboniferous boundary terrestrial extinction kill mechanism. Science Advances, 6, eaba0768.

Marynowski, L., Zatoń, M., Rakociński, M., Filipiak, P., Kurkiewicz, S., & Pearce, T. J. (2012). Deciphering the upper Famennian Hangenberg Black Shale depositional environments based on multi-proxy record. Palaeogeography, Palaeoclimatology, Palaeoecology, 346–347, 66–86.

McLennan, S. M. (2001). Relationships between the trace element composition of sedimentary rocks and upper continental crust. Geochemistry, Geophysics, Geosystems, 2, 2000GC000109.

Murchison, R. I., & Sedgwick, A. (1839). Classification of the older stratified rocks of Devonshire and Cornwall. Philosophical Magazine, ser. 3, 14, 241–260.

Nicholson, K. (1992). Contrasting mineralogical-geochemical signatures of manganese oxides: guides to metallogenesis. Economic Geology, 87, 1253–1264.

Nössing, L. (1975). Die Sanzenkogel-Schichten (Unterkarbon), eine biostratigraphische Einheit des Grazer Paläozoikums. Mitteilungen des Naturwissenschaftlichen Vereins Steiermark, 105, 79–92.

Nothdurft, L. D., Webb, G. E., & Kamber, B. S. (2004). Rare earth element geochemistry of Late Devonian reefal carbonates, Canning Basin, Western Australia: confirmation of a seawater REE proxy in ancient limestones. Geochimica et Cosmochimica Acta, 68, 263–283.

Paproth, E., Feist, R., & Flajs, G. (1991). Decision on the Devonian–Carboniferous boundary stratotype. Episodes, 14, 331–336.

Paschall, O., Carmichael, S. K., Königshof, P., Waters, J. A., Ta, P. H., Komatsu, T., & Dombrowski, A. (2019). The Devonian-Carboniferous boundary in Vietnam: sustained ocean anoxia with a volcanic trigger for the Hangenberg Crisis. Global and Planetary Change, 175, 64–81.

Percival, L. M. E., Witt, M. L. I., Mather, T. A., Hermoso, M., Jenkyns, C., Hesselbo, S. P., Al-Suwaidi, A. H., Storma, M. S., Xu, W., & Ruhla, M. (2015). Globally enhanced mercury deposition during the end-Pliensbachian extinction and Toarcian OAE: a link to the Karoo-Ferrar Large Igneous Province. Earth and Planetary Science Letters, 428, 267–280.

Plotitsyn, A. N., Zhuravlev, A. V., Sobolev, D. B., Gruzdev, D. A., Vevel, Y. A., & Nikolaeva, S. V. (2024). Devonian-Carboniferous transition in various facies of Northeast Laurussia (North Urals). Palaeoworld, 33, 1281–1297.

Préat, A., Morano, S., Loreau, J. P., Durlet, C., & Mamet, B. (2005). Petrography and biosedimentology of the Rosso Ammonitico Veronese (middle–upper Jurassic, northeastern Italy). Facies, 52, 265–278.

Přichystal, A. (1993). Paleozoic to Quaternary volcanism in the geological history of Moravia and Silesia. Geologie Moravy a Slezska, 59, 59–70.

Pujol, F., Berner, Z., & Stuben, D. (2006). Palaeoenvironmental changes at the Frasnian/Famennian boundary in key European sections: chemostratigraphic constraints. Palaeogeography, Palaeoclimatology, Palaeoecology, 240, 120–145.

Qie, W., Zhang, X., Du, Y., & Zhang, Y. (2011). Lower Carboniferous carbon isotope stratigraphy in South China: implications for the Late Paleozoic glaciations. Science China Earth Sciences, 54, 84–92.

Qie, W., Zhang, X., Du, Y., Yang, B., Ji, W., & Luo, G. (2014). Conodont biostratigraphy of Tournaisian shallow-water carbonates in central Guangxi, South China. Geobios, 47(6), 389–401.

Qie, W., Liu, J., Chen, J., Wang, X., Mii, H. S., Zhang, X., & Luo, G. (2015). Local overprints on the global carbonate δ13C signal in Devonian–Carboniferous boundary successions of South China. Palaeogeography, Palaeoclimatology, Palaeoecology, 418, 290–303.

Qie, W., Wang, X.-D., Zhang, X., Ji, W., Grossman, E. L., Huang, X., & Luo, G. (2016). Latest Devonian to earliest Carboniferous conodont and carbon isotope stratigraphy of a shallow-water sequence in South China. Geological Journal, 51, 915–935.

Qie, W., Zhang, J., Luo, G., Algeo, T. J., Chen, B., Xiang, L., et al. (2023). Enhanced continental weathering as a trigger for the end-Devonian Hangenberg Crisis. Geophysical Research Letters, 50, e2022GL102640.

Racki, G. (2020). A volcanic scenario for the Frasnian–Famennian major biotic crisis and other Late Devonian global changes: more answers than questions. Global and Planetary Change, 189, 103174.

Racki, G., Königshof, P., Bełka, Z., Dopieralska, J., & Pisarzowska, A. (2019). Diverse depositional and geochemical signatures of the Frasnian–Famennian global event in western Thailand reveal Palaeotethyan vs. Western Australian geotectonic affinities. Journal of Asian Earth Sciences: X, 2, 100010.

Racki, G. (2020). A volcanic scenario for the Frasnian–Famennian major biotic crisis and other Late Devonian global changes: more answers than questions. Global and Planetary Change, 189, 103174.

Racki, G., Königshof, P., Bełka, Z., Dopieralska, J., & Pisarzowska, A. (2019). Diverse depositional and geochemical signatures of the Frasnian–Famennian global event in western Thailand reveal Palaeotethyan vs. Western Australian geotectonic affinities. Journal of Asian Earth Sciences: X, 2, 100010.

Racki, G., Racka, M., Matyja, H., & Devleeschouwer, X. (2002). The Frasnian/Famennian boundary interval in the South Polish-Moravian shelf basins. Palaeogeography, Palaeoclimatology, Palaeoecology, 181, 251–297.

Racki, G., Rakociński, M., & Marynowski, L. (2018a). Anomalous Upper Devonian mercury enrichments: comparison of Inductively Coupled Plasma – Mass Spectrometry (ICPMS) and AAS analytical data. Geological Quarterly, 62, 487–495.

Rakociński, M., Książak, D., Pisarzowska, A., Zatoń, M., & Aretz, M. (2023). Weak and intermittent anoxia during the mid-Tournaisian (Mississippian) anoxic event in the Montagne Noire, France. Geological Magazine, 160, 831–854.

Rakociński, M., Kucharczyk, J., Pisarzowska, A., Zatoń, M., Marynowski, L., Hartenfels, S., & Becker, R. T. (2023). Redox changes and mercury signature during the Lower Alum Shale Event (mid-Tournaisian, Mississippian) in the Rhenish Massif: implications for oxygenation history and volcanism in southern Laurussian shelf and Palaeotethys Ocean. Global and Planetary Change, 227, 104165.

Rakociński, M., Marynowski, L., Zatoń, M., & Filipiak, P. (2021). The mid-Tournaisian (Early Carboniferous) anoxic event in the Laurussian shelf basin (Poland): an integrative approach. Palaeogeography, Palaeoclimatology, Palaeoecology, 566, 110236.

Rakociński, M., Pisarzowska, A., Corradini, C., et al. (2021). Mercury spikes as evidence of extended arc-volcanism around the Devonian–Carboniferous boundary in the South Tian Shan (southern Uzbekistan). Scientific Reports, 11, 5708.

Raumer, J. F., Nesbor, H.-D., & Stampfli, G. M. (2017). The north-subducting Rheic Ocean during the Devonian: consequences for the Rhenohercynian ore sites. International Journal of Earth Sciences, 106, 2279–2296.

Ricci, J., Quidelleur, X., Pavlov, V., et al. (2013). New $^{40}Ar/^{39}Ar$ and K–Ar ages of the Viluy traps (Eastern Siberia). Palaeogeography, Palaeoclimatology, Palaeoecology, 386, 531–540.

Sageman, B.B., Lyons, T.W., 2004. Geochemistry of fine-grained sediments and sedimentary rocks. In: Holland, H.D., Turekian, K.K. (Eds.), Treatise on Geochemistry, Vol. 7. Elsevier, Amsterdam, pp. 115–158.

Saltzman, M. R. (2002). Carbon and oxygen isotope stratigraphy of the Lower Mississippian (Kinderhookian–lower Osagean), western United States: implications for seawater chemistry and glaciation. Geological Society of America Bulletin, 114, 96–108.

Saltzman, M. R., González, L. A., & Lohmann, K. C. (2000). Earliest Carboniferous cooling step triggered by the Antler orogeny? Geology, 28, 347–350.

Saltzman, M.R., Thomas, E., 2012. Carbon isotope stratigraphy. In: Gradstein, F.M., Ogg, J.G., Schmitz, M.D., Ogg, G.M. (Eds.), The Geologic Time Scale 2012, Vol. 1. Elsevier, pp. 207–232.

Sandberg, C.A. & Poole, F.G., 1977. Conodont biostratigraphy and depositional complexes of Upper Devonian cratonic-platform and continental-shelf rocks in the western United States. In: Murphy, M.A. et al. (Eds.), Proceedings of the 1977 Annual Meeting of the Paleontological Society on Devonian of Western North America. University of California-Riverside, Campus Museum Contributions, no. 4, pp. 144–182.

Sandberg, C.A., Poole, F.G. & Gutschick, R.C., 1980. Devonian and Mississippian stratigraphy and conodont zonation of Pilot and Chainman shales, Confusion Range, Utah.

In: Fouch, T.D. & Magathan, E.R. (Eds.), Paleozoic Paleogeography of the West-Central United States. Rocky Mountain Paleogeography Symposium, vol. 1. Society of Economic Paleontologists and Mineralogists, Rocky Mountain Section, pp. 71–79.

Sandberg, C. A., Ziegler, W., Leuteritz, K., & Brill, S. M. (1978). Phylogeny, speciation, and zonation of Siphonodella (Conodonta, Upper Devonian and Lower Carboniferous). Newsletters on Stratigraphy, 7, 102–120.

Sanei, H., Grasby, S. E., & Beauchamp, B. (2012). Latest Permian mercury anomalies. Geology, 40, 63–66.

Schönlaub, H. P., Attrep, M., Boeckelmann, K., Dreesen, R., Feist, R., Fenninger, A., Hahn, G., Klein, P., Korn, D., Kratz, R., Magaritz, M., Orth, C. J., & Schramm, J. M. (1992). The Devonian/Carboniferous boundary in the Carnic Alps (Austria): a multidisciplinary approach. Abhandlungen der Geologischen Bundesanstalt, 135, 57–98.

Schönlaub, H. P., Feist, R., & Korn, D. (1988). The Devonian–Carboniferous boundary at the section "Grüne Schneid" (Carnic Alps, Austria): a preliminary report. Courier Forschungsinstitut Senckenberg, 100, 149–167.

Sial, A. N., Lacerda, L. D., Ferreira, V. P., Frei, R., Marquillas, R. A., Barbosa, J. A., Gaucher, C., Windmöller, C. C., & Pereira, N. S. (2013). Mercury as a proxy for volcanic activity during extreme environmental turnover: the Cretaceous–Paleogene transition. Palaeogeography, Palaeoclimatology, Palaeoecology, 387, 153–164.

Skoček, V., & Kukal, Z. (1998). Oncoidal and ooidal ironstone in the Lower Devonian limestone sequence, Barrandian, Czech Republic. Věstník Českého geologického ústavu, 73, 23–32.

Smrzka, D., Zwicker, J., Bach, W., Feng, D., Himmler, T., Chen, D., & Peckmann, J. (2019). The behavior of trace elements in seawater, sedimentary pore water, and their incorporation into carbonate minerals: a review. Facies, 65, 41.

Song, H., Jiang, G., Poulton, S. W., Wignall, P. B., Tong, J., Song, H., An, Z., Chu, D., Tian, L., She, Z., & Wang, C. (2017). The onset of widespread marine red beds and the evolution of ferruginous oceans. Nature Communications, 8, 399.

Stolfus, B. M., Cramer, B. D., Clark, R. J., Hogancamp, N. J., Day, J. E., Tassier-Surine, S. A., & Witzke, B. J. (2020). An expanded stratigraphic record of the Devonian–Carboniferous boundary Hangenberg biogeochemical event from Southeast Iowa (U.S.A.). Bulletin of Geosciences, 95, 469–495.

Tasáryová, Z., Janoušek, V., & Frýda, J. (2018). Failed Silurian continental rifting at the NW margin of Gondwana: evidence from basaltic volcanism of the Prague Basin (Teplá-Barrandian Unit, Bohemian Massif). International Journal of Earth Sciences, 107, 1231–1266.

Tostevin, R., Shields, G. A., Tarbuck, G. M., He, T., Clarkson, M. O., & Wood, R. A. (2016). Effective use of cerium anomalies as a redox proxy in carbonate-dominated marine settings. Chemical Geology, 438, 146–162.

Tribovillard, N., Algeo, T. J., Lyons, T., & Riboulleau, A. (2006). Trace metals as paleoredox and paleoproductivity proxies: an update. Chemical Geology, 232, 12–32.

Voges, A. (1959). Conodonten aus dem Untercarbon I und II (Gattendorfia- und Pericyclus-Stufe) des Sauerlandes. Palaeontologische Zeitschrift, 33, 266–314.

Walliser, O. H. (1984). Pleading for a natural D/C boundary. Courier Forschungsinstitut Senckenberg, 67, 241–246.

Webb, G. E., & Kamber, B. S. (2000). Rare earth elements in Holocene reefal microbialites: a new shallow seawater proxy. Geochimica et Cosmochimica Acta, 64, 1557–1565.

Woods, A. D. (2014). Assessing Early Triassic paleoceanographic conditions via unusual sedimentary fabrics and features. Earth-Science Reviews, 137, 6–18.

Yao, L., Aretz, M., Wignall, P. B., Chen, J., Vachard, D., Qi, Y., Shen, S., & Wang, X. (2020). The longest delay: re-emergence of coral reef ecosystems after the Late Devonian extinctions. Earth-Science Reviews, 203, 103060.

Yao, L., Qie, W., Luo, G., Liu, J., Algeo, T. J., Bai, X., Yang, B., & Wang, X. (2015). The TICE event: perturbation of carbon–nitrogen cycles during the mid-Tournaisian (Early Carboniferous) greenhouse–icehouse transition. Chemical Geology, 401, 1–14.

Zhang, K., & Shields, G. A. (2022). Sedimentary Ce anomalies: secular change and implications for paleoenvironmental evolution. Earth-Science Reviews, 229, 104015.

Zhang, K., & Shields, G. A. (2023). Early diagenetic mobilization of rare earth elements and implications for the Ce anomaly as a redox proxy. Geochimica et Cosmochimica Acta, 355, 271–288.

Zhuravlev, A. V. (2007). Zonal scheme of the Tournaisian stage based on conodonts. Upper Palaeozoic of Russia, 110, 110–112.

Ziegler, W. (1971). Conodont stratigraphy of the European Devonian. Geological Society of America Memoir, 127, 227–284.

Ziegler, W., & Sandberg, C. A. (1996). Reflections on Frasnian and Famennian stage boundary decisions as a guide to future deliberations. Newsletters on Stratigraphy, 33, 157–180.

Zwicker, J., Smrzka, D., Himmler, T., Monien, P., Gier, S., Goedert, J. L., & Peckmann, J. (2018). Rare earth elements as tracers for microbial activity and early diagenesis: a new perspective from carbonate cements of ancient methane-seep deposits. Chemical Geology, 501, 83–97.

Appendix A Attached Commented Articles